

Diplomarbeit

zur Erlangung des akademischen Grades einer
Magistra der Naturwissenschaften

Correlations in ultracold Bose-Einstein condensates

Autorin: Miriam Mutici

Betreuer: Ao. Univ. Prof. Mag. Dr. Ulrich Hohenester

Institut für Physik, Fachbereich Theoretische Physik
Karl-Franzens-Universität Graz



2013

Abstract

The aim of this thesis is to find a model that describes the generation of twin-atom beams emitted from a quasi Bose-Einstein condensate. Our work is motivated by an experiment performed by a group from the *Institute of Atomic and Subatomic Physics* at the *Vienna University of Technology* and was published in [1].

Starting point for the generation of twin-atom beams is a one-dimensional, degenerate Bose gas trapped in the ground state of an elongated magnetic potential. This quasi-condensate is transferred to the first radial excited state by shaking the trap. Subsequently, pairs of atoms with opposite momenta are emitted from the source and propagate in longitudinal direction.

To model this behavior, we use a density matrix approach which is first applied to a simplified two-mode model of the emission process. We probe different factorization schemes, a pseudospin-operator ansatz, and a coupled-cluster approach, and compare the results to the one obtained by the exact solution of the full Schrödinger equation. Then we use the first-order approximation within the density matrix approach and generalize it to a multi-mode model. We allow several twin-modes to be populated and also imply the pumping-process in our simulation, finding good agreement with the experiment.

Contents

1	Bose-Einstein condensation	1
1.1	Definitions	1
1.2	The condensate wave function	2
1.3	Gross-Pitaevskii equation	3
2	Bose-Einstein condensation in lower dimensions	4
3	Experimental realization of BEC	6
3.1	Atom chips	8
4	Twin-atom beams: The experiment	9
5	General theory of many-body physics	12
5.1	The general many-body Hamiltonian	12
5.2	Density-matrix formalism	13
6	Twin-atom beams: The theory	14
6.1	The model	14
6.2	Calculating the ground state	14
6.3	Two-mode model	16
6.3.1	The Hamiltonian	16
6.3.2	Full solution of the Schrödinger equation	16
6.3.3	Density matrix approach	18
6.3.4	Pseudospin-operator approach	22
6.4	Truncation of the hierarchy of expectation value equations of motion	25
6.4.1	Two-mode model of a condensate in a double well trap	25
6.4.2	Comparison of the two-mode models of a condensate in double well versus that of twin-atom beam generation	26
6.5	Coupled-cluster approximation	27
6.5.1	Basics of the coupled-cluster theory	27
6.5.2	Application of coupled-cluster theory to the generation of twin-atom beams	29
6.6	Multi-mode model	32
6.7	Conclusion and outlook	34
	Appendices	39
	Appendix A Heisenberg equations of motion	39
A.1	Two-mode model	39
A.1.1	First-order approximation	39
A.1.2	Second-order approximation	41
A.1.3	Pseudospin-operator approach	42
A.2	Multi-mode model	44
A.2.1	Pumping and free time evolution	44

A.2.2	Twin-atom beam generation	46
Appendix B	Coupled-cluster theory	48
B.1	Expectation values of excitation operators	48

1 Bose-Einstein condensation

1.1 Definitions

Bose-Einstein condensation (BEC) occurs when a single quantum state becomes occupied in a macroscopic way. This is the definition made by A. Einstein in 1924–25 considering ideal gases [2, 3]. With further investigation, also of interacting and nonuniform Bose gases, a more precise formulation became necessary.

If we formalize the original definition its deficiencies become obvious. As the system shows BEC when the number of particles condensed in the ground state N_0 is proportional to the total number of particles N , in the thermodynamic limit, the condition can be written as

$$\lim_{N \rightarrow \infty} \frac{N_0}{N} > 0. \quad (1)$$

While for the ideal gas the macroscopically occupied single-particle state is well defined, there is an ambiguity in the choice of a single-particle basis in the case of interacting particles. Therefore the ground state and its occupation number are not uniquely defined in this case [4]. Furthermore, this formulation does not provide the occurrence of a fragmented BEC, where several states become occupied macroscopically [5]. Penrose and Onsager [4] generalized this criterion and made it applicable also to interacting particles. For that purpose, the one-body density matrix

$$\rho^{(1)}(\mathbf{r}, \mathbf{r}') \equiv \langle \hat{\Psi}^\dagger(\mathbf{r}) \hat{\Psi}(\mathbf{r}') \rangle \quad (2)$$

is defined, where $\hat{\Psi}^\dagger(\mathbf{r})$ ($\hat{\Psi}(\mathbf{r})$) is the field operator creating (annihilating) a particle at the point \mathbf{r} . The boson field operators satisfy the usual commutation relations

$$[\hat{\Psi}(\mathbf{r}), \hat{\Psi}^\dagger(\mathbf{r}')] = \delta(\mathbf{r} - \mathbf{r}'), \quad [\hat{\Psi}(\mathbf{r}), \hat{\Psi}(\mathbf{r}')] = 0 \quad (3)$$

The eigenvalues γ_n of this matrix $\rho^{(1)}$ are defined by the solution of the eigen equation

$$\int \rho^{(1)}(\mathbf{r}, \mathbf{r}') \varphi_n(\mathbf{r}') d\mathbf{r}' = \gamma_n \varphi_n(\mathbf{r}). \quad (4)$$

Now the criterion (1) can be rewritten in terms of the largest eigenvalue as

$$\lim_{N \rightarrow \infty} \frac{\sup_n \gamma_n}{N} > 0. \quad (5)$$

Since the density matrix $\rho^{(1)}$ is well defined for both noninteracting and interacting particles, this formulation is valid in either case.

An alternative way to formulate the condition for BEC is to require off-diagonal long-range order (ODLRO). A system exhibits ODLRO if the one-body density matrix $\rho^{(1)}(\mathbf{r}, \mathbf{r}')$ has a non-vanishing value. Also at large values

of separation $|\mathbf{r} - \mathbf{r}'|$. This can be written as the limit

$$\lim_{|\mathbf{r}-\mathbf{r}'|\rightarrow\infty} \rho^{(1)}(\mathbf{r}, \mathbf{r}') = \Psi_0^*(\mathbf{r})\Psi_0(\mathbf{r}') \equiv \rho_0 > 0 \quad (6)$$

where $\Psi_0(\mathbf{r})$ is called the *condensate wave function* or the *order parameter* and ρ_0 is the condensate density. Since the density matrix is hermitian, it can be written in the diagonalized form

$$\rho^{(1)}(\mathbf{r}, \mathbf{r}') = \sum_n \gamma_n \varphi_n^*(\mathbf{r}) \varphi_n(\mathbf{r}'). \quad (7)$$

If Bose-Einstein condensation occurs, one single-particle state gets macroscopically occupied. In the following, this state will be called $\varphi_0(\mathbf{r})$. In the above expansion, the term containing this single-particle state $\varphi_0(\mathbf{r})$ and its corresponding macroscopic eigenvalue γ_0 , provide the main contribution to that sum and

$$\rho^{(1)}(\mathbf{r}, \mathbf{r}') \simeq \gamma_0 \varphi_0^*(\mathbf{r}) \varphi_0(\mathbf{r}'). \quad (8)$$

Hence, the macroscopically occupied single-particle state can be identified with the condensate wave function, i.e.

$$\Psi_0(\mathbf{r}) = \sqrt{N_0} \varphi_0(\mathbf{r}) \quad (9)$$

where $N_0 \equiv \gamma_0$ is the largest eigenvalue of the density matrix.

While in the case of an ideal gas, where $\varphi_0(\mathbf{r})$ is the zero-momentum state, the condition for ODLRO (6) is fulfilled, it has to be weakened for confined systems. This means, that both \mathbf{r} and \mathbf{r}' must remain within the atomic cloud, since all single-particle wave functions $\varphi_n(\mathbf{r})$ tend to zero as $\mathbf{r} \rightarrow \infty$. Thus, strictly speaking, finite sized systems do not show ODLRO.

1.2 The condensate wave function

An alternative way to deduce the condensate wave function starts with writing the field operator in terms of the single-particle states φ_i as

$$\hat{\Psi}(\mathbf{r}) = \sum_i \hat{a}_i \varphi_i(\mathbf{r}) \quad (10)$$

where \hat{a}_i is the annihilation operator for a particle in the state φ_i , and \hat{a}_i^\dagger is the corresponding creation operator. In Fock space these operators are defined as

$$\hat{a}_i^\dagger |n_0, n_1, \dots, n_i, \dots\rangle = \sqrt{n_i + 1} |n_0, n_1, \dots, n_i + 1, \dots\rangle \quad (11)$$

$$\hat{a}_i |n_0, n_1, \dots, n_i, \dots\rangle = \sqrt{n_i} |n_0, n_1, \dots, n_i - 1, \dots\rangle \quad (12)$$

where $n_i = \langle \hat{a}_i^\dagger \hat{a}_i \rangle$ is the number of particles in the state φ_i and the operators obey the commutation relations

$$[\hat{a}_i, \hat{a}_j^\dagger] = \delta_{ij}, \quad [\hat{a}_i, \hat{a}_j] = 0, \quad [\hat{a}_i^\dagger, \hat{a}_j^\dagger] = 0. \quad (13)$$

If BEC occurs, the occupation number of one single-particle state ($i = 0$) becomes very large. In the expansion (10) the condensate contribution, containing the corresponding single-particle wave function, can be separated out. Thus the field operator can be written as

$$\hat{\Psi}(\mathbf{r}) = \hat{a}_0\varphi_0(\mathbf{r}) + \sum_{i \neq 0} \hat{a}_i\varphi_i(\mathbf{r}). \quad (14)$$

Since the number of condensed particles $N_0 \equiv \langle \hat{a}_0^\dagger \hat{a}_0 \rangle \gg 1$ the non-commutativity of \hat{a}_0 and \hat{a}_0^\dagger can be neglected, which corresponds to replacing the operators \hat{a}_0 and \hat{a}_0^\dagger by the c-number $\sqrt{N_0}$. This approach, known as the *Bogoliubov approximation*, allows one to write the field operator as

$$\hat{\Psi}(\mathbf{r}) = \Psi_0(\mathbf{r}) + \tilde{\Psi}(\mathbf{r}), \quad (15)$$

where the complex function $\Psi_0(\mathbf{r}) = \sqrt{N_0}\varphi_0(\mathbf{r})$ is the wave function of the condensate, as it was already stated in (9), and $\tilde{\Psi}(\mathbf{r})$ describes the bosons outside the condensate. From (14) one can see that, due to the Bogoliubov approximation, $\langle \Psi_0(\mathbf{r}) \rangle \neq 0$, while for the non-condensate component $\langle \tilde{\Psi}(\mathbf{r}) \rangle = 0$. Thus

$$\Psi_0(\mathbf{r}) = \langle \hat{\Psi}(\mathbf{r}) \rangle. \quad (16)$$

1.3 Gross-Pitaevskii equation

The Hamiltonian for a system of N interacting bosons, trapped by an external potential V_{trap} reads

$$\begin{aligned} \hat{H} = & \int d\mathbf{r} \hat{\Psi}^\dagger(\mathbf{r}, t) \left[-\frac{\hbar^2}{2m} \nabla^2 + V_{\text{trap}}(\mathbf{r}, t) \right] \hat{\Psi}(\mathbf{r}, t) \\ & + \frac{1}{2} \int d\mathbf{r} \int d\mathbf{r}' \hat{\Psi}^\dagger(\mathbf{r}, t) \hat{\Psi}^\dagger(\mathbf{r}', t) V(\mathbf{r} - \mathbf{r}') \hat{\Psi}(\mathbf{r}', t) \hat{\Psi}(\mathbf{r}, t), \end{aligned} \quad (17)$$

where $\hat{\Psi}(\mathbf{r}, t)$ is the boson field operator and $V(\mathbf{r} - \mathbf{r}')$ is the two-body interaction potential. Collisions of three or more particles can be neglected because of the very low density of the gas. From this Hamiltonian we get the following Heisenberg equation of motion for the field operator $\hat{\Psi}(\mathbf{r}, t)$

$$\begin{aligned} i\hbar \frac{\partial}{\partial t} \hat{\Psi}(\mathbf{r}, t) = & \left[\hat{\Psi}(\mathbf{r}, t), \hat{H} \right] = \\ = & \left[-\frac{\hbar^2}{2m} \nabla^2 + V_{\text{trap}}(\mathbf{r}, t) + \int d\mathbf{r}' \hat{\Psi}^\dagger(\mathbf{r}', t) V(\mathbf{r} - \mathbf{r}') \hat{\Psi}(\mathbf{r}', t) \right] \hat{\Psi}(\mathbf{r}, t), \end{aligned} \quad (18)$$

where the commutation relations (3) for the field operator have been used. This equation in general cannot be solved. Therefore a mean-field approach is taken, where one makes use of the decomposition (15). If the depletion of the condensate is small, the non-condensate term $\tilde{\Psi}$ can be neglected and the

field operator in (18) can be substituted by the condensate wave function Ψ_0 . However, the use of the interatomic potential $V(\mathbf{r} - \mathbf{r}')$ is no longer adequate and has to be replaced by an effective soft potential that possesses the same s-wave scattering length. The s-wave scattering length a is the parameter that solely characterizes the interatomic interaction. This yields

$$i\hbar \frac{\partial}{\partial t} \Psi_0(\mathbf{r}, t) = \left[-\frac{\hbar^2}{2m} \nabla^2 + V_{\text{trap}}(\mathbf{r}, t) + \int d\mathbf{r}' \Psi_0^\dagger(\mathbf{r}', t) V_{\text{eff}}(\mathbf{r} - \mathbf{r}') \Psi_0(\mathbf{r}', t) \right] \Psi_0(\mathbf{r}, t). \quad (19)$$

Since Ψ_0 varies slowly on the length scales of the range of the interatomic force, one can replace \mathbf{r}' by \mathbf{r} in the argument of Ψ_0 in the integral in the above equation and one gets

$$i\hbar \frac{\partial}{\partial t} \Psi_0(\mathbf{r}, t) = \left(-\frac{\hbar^2}{2m} \nabla^2 + V_{\text{trap}}(\mathbf{r}, t) + g |\Psi_0(\mathbf{r}, t)|^2 \right) \Psi_0(\mathbf{r}, t), \quad (20)$$

with the interaction coupling constant being fixed by the s-wave scattering length a through $g = \frac{4\pi\hbar^2 a}{m}$. This equation is known as the *Gross-Pitaevskii equation* (GPE) and was derived independently by Gross[6] and Pitaevskii [7] in 1961. Here the order parameter is normalized to the total number of particles, i.e. $\int d\mathbf{r} |\Psi_0|^2 = N$, and thus the condensate density is given by $\rho(\mathbf{r}) = |\Psi_0(\mathbf{r})|^2$.

Within mean-field theory, the ground state of a BEC can be calculated from the time-independent GPE, which is obtained by substituting

$$\Psi_0(\mathbf{r}, t) = \Psi_0(\mathbf{r}) \exp\left(-\frac{i\mu t}{\hbar}\right) \quad (21)$$

for the condensate wave function into (20). The time evolution is fixed by the chemical potential $\mu = \frac{\partial E}{\partial N}$. This leads to

$$\left(-\frac{\hbar^2}{2m} \nabla^2 + V_{\text{trap}}(\mathbf{r}) + g |\Psi_0(\mathbf{r})|^2 \right) \Psi_0(\mathbf{r}) = \mu \Psi_0(\mathbf{r}), \quad (22)$$

which is called the *stationary Gross-Pitaevskii equation*.

2 Bose-Einstein condensation in lower dimensions

The investigation of Bose gases in lower dimensions is of great interest because the underlying physics is very different from that of a three-dimensional gas. For example, the one-dimensional trapped gas of interacting bosons shows quantum statistics which, depending on the temperature and the number of atoms, can be of bosonic, classical or fermionic character [8].

Experimentally such a highly anisotropic configuration can be realized by choosing the shape of the trapping potential in a way that allows to tightly confine the motion of the trapped atoms in one or two directions to zero point oscillations. The first experimental realization of a BEC in lower dimensions was done by Görlitz *et al.* in 2001 [9]. Based on a changed behavior of the released atoms, a crossover from a 3D to a 2D and 1D condensate was observed. For a reduced number of particles the aspect ratio changes and, unlike in 3D condensates, the release energy no longer depends on the number of particles but tends to a non-zero value in lower dimensions.

Long before the realization of these experiments condensation in lower-dimensional Bose gases has already been investigated theoretically. Due to the Mermin-Wagner-Hohenberg theorem [10, 11], a homogeneous one-dimensional Bose gas cannot exhibit BEC at all temperatures [12], whereas a homogeneous two-dimensional system only does at $T = 0$. For trapped Bose gases, however, the situation is different and the criteria for BEC have to be redefined. In this manner, a finite, inhomogeneous system can exhibit BEC because the trapping potential changes the density of states [13].

In the case of an ideal Bose gas this can be easily understood: In the context of the grand canonical ensemble the total number of particles of the uniform d -dimensional Bose gas is given by

$$N = \sum_{\mathbf{k}} \frac{1}{e^{\beta(\epsilon_{\mathbf{k}} - \mu)} - 1} \quad (23)$$

where $\beta = \frac{1}{k_B T}$, $\epsilon_{\mathbf{k}} = \frac{\hbar^2 k^2}{2m}$ and μ is the chemical potential. This sum can be written as an integral, which yields

$$N = N_0 + \int_0^\infty d\epsilon \frac{\rho(\epsilon)}{e^{\beta(\epsilon - \mu)} - 1} \quad (24)$$

where $\rho(\epsilon)$ is the density of states, that is $\rho(\epsilon) \propto \epsilon^{d/2-1}$, and N_0 is the number of particles condensed into the ground state, which is mentioned explicitly since $\rho(0) = 0$. If at $T = T_C$ BEC occurs, this integral has a finite value at $\mu = 0$. It is easy to see that this integral diverges for small values of ϵ in the case of a two-dimensional Bose gas, where the density of states is constant. A divergence also occurs for the one-dimensional case, where the density is proportional to $\frac{1}{\sqrt{\epsilon}}$. However, the density of states changes if the gas is no longer uniform. In the presence of a harmonic potential the density of states is given by $\rho(\epsilon) \propto \epsilon^{d-1}$ and the integral in (24) converges for the case of a two-dimensional system. But the one-dimensional Bose gas cannot exhibit BEC even if there is a harmonic confinement potential, because the integral in (24) is still divergent. This means that in the thermodynamic limit, where $N \rightarrow \infty$ and $\omega_{1D} \rightarrow 0$ with $N\omega_{1D}$ kept fixed, the critical temperature tends to zero. In general experiments are performed with a finite number of particles and the thermodynamic limit is not fully justified. However, for finite systems one does not speak of a phase transition. Yet, a quasi-condensation can occur, where the lowest single-particle state is substantially occupied. A one-dimensional trapped Bose gas shows this BEC-like behavior below a critical temperature of $T_C^{1D} k_B = \hbar\omega_{1D} \frac{N}{\ln(2N)}$ [14].

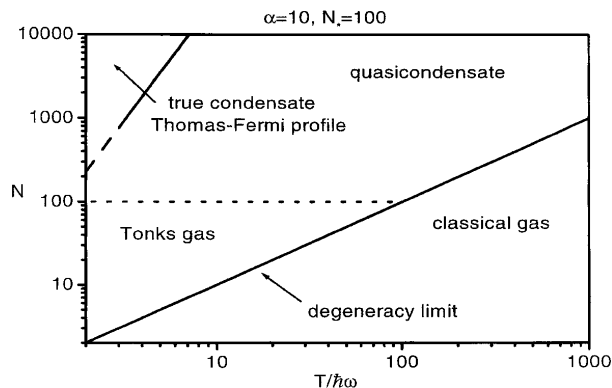


Figure 1: Diagram of states for a trapped 1D gas at finite temperature taken from [8].

Furthermore, the inter-particle interactions play an important role. The case of the trapped interacting Bose gas was investigated by Petrov *et al* [8]. They identified three regimes of quantum degeneracy: that of a quasi-condensate (with fluctuating phase), that of a true condensate and that of a trapped Tonks gas, which is a gas of impenetrable bosons that shows a Fermi-gas density profile.

3 Experimental realization of BEC

To understand how a BEC is created we take a look at the main steps of a typical experiment. First, atoms are heated in an oven and emerge as a beam. These hot, and thus very fast atoms are then slowed down in a so called Zeeman slower. There the atoms absorb photons from a counter-propagating laser beam and thereby reduce their velocity due to an exchange of momentum with the photons. When the excited atoms re-emit the photons subsequently, they do this in a random direction and so this process does not change the average speed. Therefore, considering the total process of the atom absorbing and emitting a photon, the average speed is decreased. Since the atoms' velocities follow a Maxwell distribution, only atoms with a certain velocity are resonant to the photons frequency and can therefore be cooled (see figure 2). To achieve a cooling even of the atoms with different velocities, an inhomogeneous magnetic field induces a Zeeman shift of the atoms' frequencies. The atoms leave the Zeeman slower with a speed one order of magnitude smaller and are now slow enough to be captured by a magneto-optical trap (MOT) [15] where they are further cooled by the radiation pressure of several laser beams to temperatures of order $100\mu K$. To avoid diffusion of the atoms, a spatially varying magnetic field and the accompanying Zeeman effect are used to generate a position-dependent force that keeps the atoms inside the trap. The temperatures that can be

reached with optical cooling are limited by the heating, caused by spontaneous emission. To reach temperatures low enough to achieve BEC further cooling is necessary. Therefore the laser beams of the MOT are turned off when a sufficiently large number of atoms has accumulated and the atoms are transferred to a solely magnetic trap, where they are confined in a minimum and the temperature can be further decreased by evaporative cooling. Within this technique, the highest energy atoms are removed from the trap and the mean energy, i.e. the temperature of the remaining atoms is reduced. Moreover also the phase space density is increased by this process and finally the conditions for BEC can be reached by this combination of laser cooling, magnetic trapping and evaporative cooling.

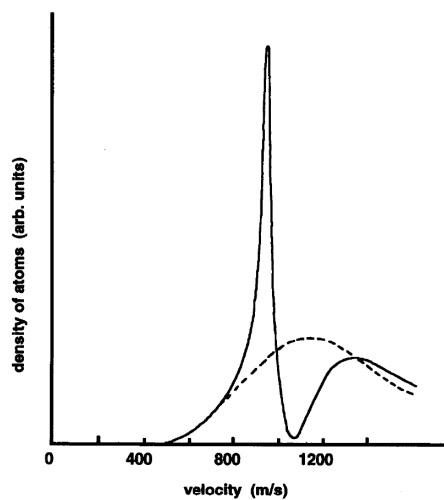


Figure 2: Figure from the 1997 Nobel lecture by W. D. Phillips [16] showing the velocity distribution of atoms before (dashed line) and after (solid line) laser cooling at a fixed frequency.

To measure the density distribution of the atoms in the condensate, several imaging techniques exist. The most popular method is *absorption imaging* [17], where a laser beam, with a frequency resonant to an atomic transition, is passed through the atomic cloud. Thereby an absorption profile occurs, which is measured with a CCD and gives information on the spatial density distribution. To improve the spatial resolution, the cloud is released from the trap and freely expands before imaging, this is called a *time-of-flight* imaging technique. Another technique, which also works for very low densities, is *fluorescence imaging* [18], where the atoms of the expanding cloud are excited when falling through a thin *light sheet*, and the emitted fluorescence photons are measured (see schematic in figure 7). However, these kinds of measurements destroy the BEC and to observe a time-dependent process it is therefore necessary to make measurements of different condensates released at different times.

fabricated with lithographic techniques. The simplest micro-trap geometry is that of a straight conducting wire combined with a homogeneous magnetic field perpendicular to the wire (figure 4). In this configuration the external magnetic field cancels with that of the wire in a line parallel to the conductor in a certain distance d off the wire. There a minimum of the magnetic field occurs, where the *low-field seekers* can be trapped. However, in regions of a vanishing magnetic field the adiabatic approximation used in (25) is no longer valid, and the internal atomic states can change. Thus *low-field seekers* can turn to *strong-field seekers* and escape from the trap, this effect is known as *Majorana loss* and can be avoided by adding an additional homogeneous magnetic field parallel to the wire, what leads to a non-vanishing magnetic field in the minimum giving a *Ioffe-Pritchard type trap*. One way to get such an additional parallel magnetic field is to use a wire in Z-shape instead of a straight one (see [23] for an overview of different trap types).

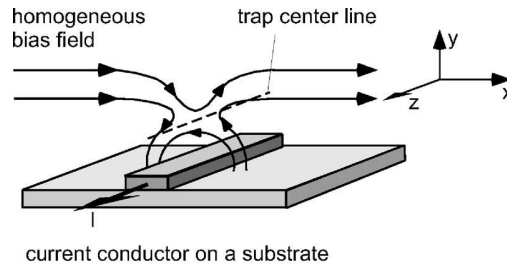


Figure 4: A simple magnetic trap, where the atoms accumulate in minimum of the magnetic potential (dashed line), which forms in a straight line above the conducting wire, where the external homogeneous magnetic field cancels with that of the conducting wire (illustration from [23]).

The strength of the magnetic confinement depends on the field gradient near the minimum, which increases as $1/d^2$ when reducing the distance d to the wire as long as this distance is larger than the diameter of the wire. Hence bringing atoms closer to the chip surface and making the wires smaller leads to a stronger confinement, thus allowing faster evaporative cooling and a BEC can be formed more quickly [24].

4 Twin-atom beams: The experiment

While in light optics a laser beam is an electromagnetic wave, propagating in a single mode, the analogy in matter wave physics can, at least for bosons, be realized by a BEC, where all atoms occupy a single mode. By the manipulation of these BECs matter-wave optic experiments can be realized. One experiment already accomplished is beam-splitting, for BECs, performed by the change of a harmonic to a double-well trapping potential on an atom chip [25]. After coherent splitting, the condensates are released and an interference can be observed.

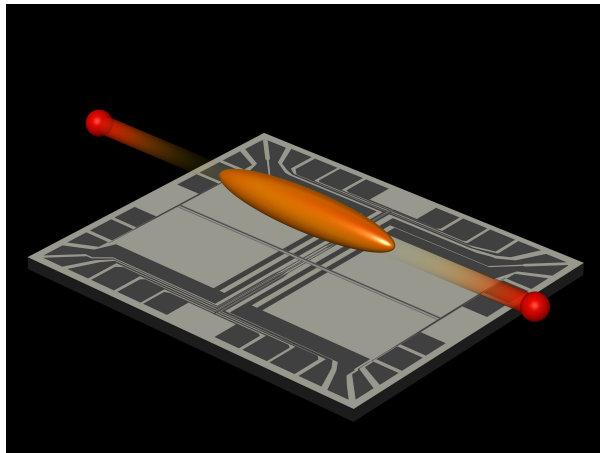


Figure 5: Emission of a pair of twin-atoms from a quasi-BEC taken from [26].

Another experiment already established in light optics is the generation of twin-photon beams [27]. In the experiment, which is the basis for the model developed within this thesis, the matter-wave analog, the generation of twin-atom beams [1], was realized. The starting point for this twin-atom beam generation is a one-dimensional quantum-degenerate Bose gas, which is generated from a gas of neutral Rubidium 87 atoms on an *atom chip* with techniques described in the previous sections. There are typically 700 atoms magnetically trapped in a highly elongated potential, with a tight radial confinement (in the y,z -plane) and a shallow confinement in the axial direction ($\nu_x = 16.3\text{Hz}$). These atoms are cooled to a temperature of $T \lesssim 35\text{nK} \approx h k_B \cdot 730\text{Hz}$. In the radial plane anharmonic potentials establish an effective two-level system consisting of the ground state $|0,0\rangle$ and the first excited state along the y -direction $|1_y,0\rangle$. The potential in y -direction, along which the excitation takes place, can be approximated by a quadratic polynomial of the form

$$E_y = h \cdot 13.1\text{Hz} \left(\frac{r}{r_0}\right)^4 + h \cdot 343\text{Hz} \left(\frac{r}{r_0}\right)^2 \quad (26)$$

and the one in z -direction, perpendicular to the excitation motion by

$$E_z = h \cdot 10.4\text{Hz} \left(\frac{r}{r_0}\right)^4 + h \cdot 793\text{Hz} \left(\frac{r}{r_0}\right)^2 \quad (27)$$

where $r_0 = 172\text{nm}$ is the mean radial ground state radius. The first excited single-particle state $|1_y,0\rangle$, has an energy of $E_{y,z}^{(1)} = h \cdot [1.83, 2.58]$. The chemical potential, that quantifies the mean-field interaction, is given by $\mu \sim h \cdot 500\text{Hz} \ll E_y^{(1)}$. Because $k_B T, \mu < h\nu_\perp$ and $\nu_x \ll \nu_\perp$ the system is a one-dimensional, weakly-interacting quasi-BEC [8].

This quasi-BEC in the radial ground state can be transferred to the first excited state by transversal shaking of the trap. This happens with an efficiency of 97% by displacing the radial trap minimum along an optimized trajectory.

This trajectory is calculated numerically by using Optimal Control Theory of the 1D-GPE, a technique already used before in theoretical works on transferring and splitting a BEC [28]. The one-dimensional approximation, performed along the y -direction, is justified, as the dynamics in the axial direction is much slower than in the radial ones, and the z -direction is not significantly affected by the displacement of the minimum. Furthermore two-dimensional simulations just lead to small deviations compared to the one-dimensional case.

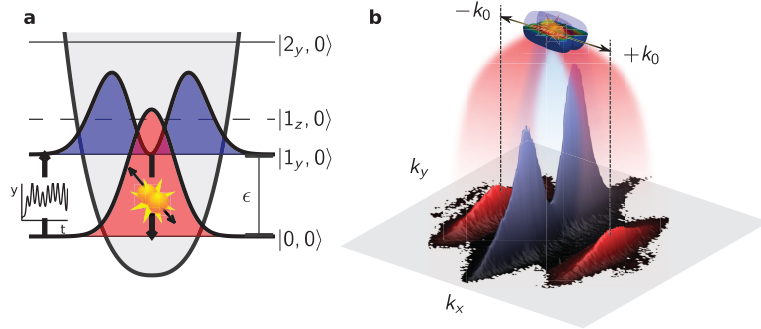


Figure 6: Schematic of the excitation and emission process from [1].

After excitation atom pairs undergo collisional relaxation. Due to parity conservation, relaxation is just possible into a single transverse state, namely the radial ground state, and because of momentum conservation the atoms obtain a momentum of $\pm k$ in axial direction. Twin-atoms in the $|0, \pm k\rangle$ modes are created, depleting the first excited state $|1_y, 0\rangle$ (see figure 6).

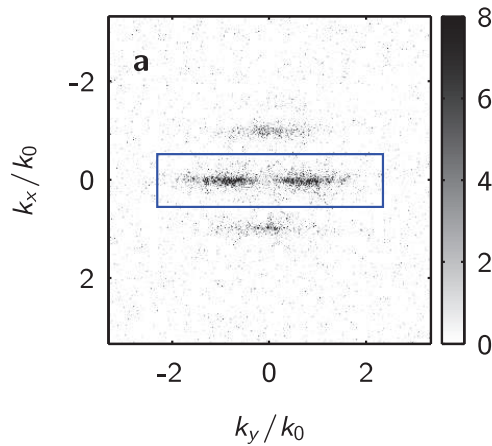


Figure 7: Momentum distribution of about 700 atoms, 7 ms after starting the excitation sequence from [1].

The atoms in the $|0, \pm k\rangle$ can be observed by *single-atom-sensitive fluorescence imaging* (see chapter 3). In figure 7, the momentum distribution of about 700 atoms, 7 ms after starting the excitation sequence is shown. It is calculated

from the information gained by using fluorescence imaging on the atom cloud after 46 ms of expansion. From measurements at different release times also the time-dependence of the population of the emitted clouds can be calculated, what is shown in figure 8. Since the model, taking only spontaneous processes into account, is obviously not adequate to describe the emission process, a better approach has to be found, as will be developed in this thesis.

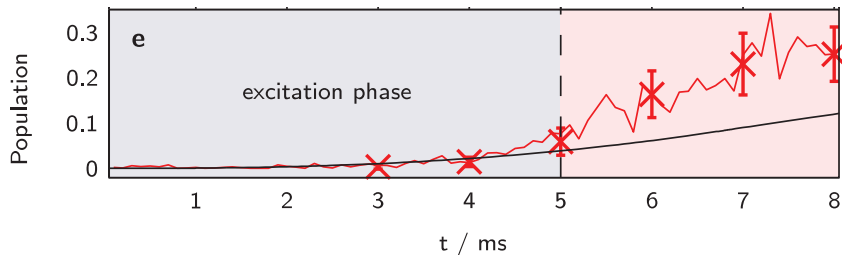


Figure 8: Measured population of the wing states (red line) and theoretical estimation for spontaneous processes only (black line) from [1].

Also the number fluctuation between the beams was measured and a non-classical suppression was observed.

5 General theory of many-body physics

5.1 The general many-body Hamiltonian

A system of N spinless, pairwise interacting bosons can be described by a Hamiltonian, which in second quantized form reads

$$\hat{H} = \int d\mathbf{r} \hat{\Psi}^\dagger(\mathbf{r}) h(\mathbf{r}, t) \hat{\Psi}(\mathbf{r}) + \frac{1}{2} \int d\mathbf{r} \int d\mathbf{r}' \hat{\Psi}^\dagger(\mathbf{r}) \hat{\Psi}^\dagger(\mathbf{r}') V(\mathbf{r} - \mathbf{r}') \hat{\Psi}(\mathbf{r}) \hat{\Psi}(\mathbf{r}') \quad (28)$$

where $\hat{\Psi}(\mathbf{r}, t)$ is the boson field operator, $V(\mathbf{r} - \mathbf{r}')$ is the two-body interaction potential and

$$h(\mathbf{r}, t) = -\frac{\hbar^2}{2m} \nabla^2 + V_{\text{trap}}(\mathbf{r}) \quad (29)$$

is the one-body Hamiltonian containing the kinetic energy and the trapping potential $V_{\text{trap}}(\mathbf{r})$. The field operators obey the usual bosonic commutation relations and can be written as the expansion

$$\hat{\Psi}(\mathbf{r}) = \sum_{k=1}^{\infty} \hat{a}_k(t) \phi_k(\mathbf{r}, t) \quad (30)$$

where the set $\{\phi_k\}$ of single-particle functions, which in this context are called *orbitals*, form an orthonormal basis and \hat{a}_k (\hat{a}_k^\dagger) are the corresponding annihilation (creation) operators obeying the equal-time commutation relations for

bosons. The field operators in the many-body Hamiltonian are now substituted by their expansions giving

$$\hat{H} = \sum_{k,q} \hat{a}_k^\dagger(t) \hat{a}_q(t) h_{kq}(t) + \frac{1}{2} \sum_{k,s,q,l} \hat{a}_k^\dagger(t) \hat{a}_s^\dagger(t) \hat{a}_q(t) \hat{a}_l(t) V_{ksql}(t), \quad (31)$$

with

$$h_{kq}(t) = \int d\mathbf{r} \phi_k^*(\mathbf{r}, t) h(\mathbf{r}, t) \phi_q(\mathbf{r}, t) \quad (32)$$

$$V_{ksql}(t) = \int d\mathbf{r} \int d\mathbf{r}' \phi_k^*(\mathbf{r}, t) \phi_s^*(\mathbf{r}', t) V(\mathbf{r} - \mathbf{r}') \phi_q(\mathbf{r}, t) \phi_l(\mathbf{r}', t). \quad (33)$$

In the case of an effectively weak atom-atom interaction, which is dominated by s-wave scattering, only binary collisions have to be considered and the interaction potential can be approximated by

$$V(\mathbf{r} - \mathbf{r}') = g\delta(\mathbf{r} - \mathbf{r}'), \quad (34)$$

where the coupling constant is fixed by the s-wave scattering length. In this approximation, the interaction matrix elements are given by

$$V_{ksql}(t) = g \int d\mathbf{r} \phi_k^*(\mathbf{r}, t) \phi_s^*(\mathbf{r}, t) \phi_q(\mathbf{r}, t) \phi_l(\mathbf{r}, t). \quad (35)$$

5.2 Density-matrix formalism

To calculate the dynamics of a N -particle system we can introduce the reduced single-particle density matrix (SPDM) ρ with the elements $\rho_{ij} = \frac{1}{N} \langle \hat{a}_i^\dagger \hat{a}_j \rangle$ and calculate their time evolution by setting up the Heisenberg equations of motion $i \frac{d}{dt} \rho_{ij} = \langle [\hat{a}_i^\dagger \hat{a}_j, \hat{H}] \rangle$. For a non-linear Hamiltonian these equations also depend on the two-particle density matrix $\Delta_{ij,kl} = \frac{1}{N^2} \langle \hat{a}_i^\dagger \hat{a}_j^\dagger \hat{a}_k \hat{a}_l \rangle$. The equations of motion for the two-particle density matrix similarly depend on the three-particle density matrix and so on. The arising hierarchy is known as the BBGKY (Bogoliubov-Born-Green-Kirkwood-Yvon) hierarchy of equations of motions and is finite for a system with a fixed finite number of particles. Since the number of particles N can be huge, a truncation of the hierarchy becomes necessary to obtain a closed set of equations. To lowest order, the two-particle density matrix elements can be approximated by products of single-particle matrix elements what is achieved by applying the factorization $\langle \hat{a}_i^\dagger \hat{a}_j^\dagger \hat{a}_k \hat{a}_l \rangle \simeq \langle \hat{a}_i^\dagger \hat{a}_k \rangle \langle \hat{a}_j^\dagger \hat{a}_l \rangle - \delta_{jk} \langle \hat{a}_i^\dagger \hat{a}_l \rangle$ to the two-particle density matrix elements. This truncation corresponds to a mean-field approach. In some cases, this is not sufficient to describe a system adequately as we will notice in the following sections and will therefore have to apply a higher order approximation.

6 Twin-atom beams: The theory

6.1 The model

The system under consideration is a one-dimensional, weakly interacting quasi-BEC [1] that is formed by a magnetic trap providing tight radial (x-y-plane) and weak axial confinement (x-direction). A quasi-BEC in the radial ground state with zero momentum along the longitudinal direction is prepared $(g, 0)$ and subsequently excited into the radial first excited state $(e, 0)$ by transverse shaking of the trap. The shaking is realized by a displacement of the trap-minimum along the y-direction. This is implemented by a time-dependent potential $V_y(y - y_0(t))$. Since the potential is sufficiently anisotropic also in the radial plane, the z-direction is not significantly affected by the movement. Hence, the state $(e, 0)$ is the first excited state along the y-direction. Once excited in the $(e, 0)$ state, atoms in the quasi-BEC undergo collisional relaxation into the radial ground state. Thereby, two-particle collisions create twin atoms in the modes $(g, \pm p)$, with opposite finite momenta along the longitudinal direction. In a first approach we will assume that, due to energy conservation, these are states with energies $E_{g, \pm p} = E_{e, 0}$. Hence we are left with a two-mode model for the emission process, including only the states $(e, 0)$ and $(g, \pm p)$. This is implemented in chapter 6.3. Furthermore, in section 6.6, we will develop a multi-mode model which takes into account the scattering to several modes $(g, \pm p_i)$ with energies $E_{g, \pm p_i} \simeq E_{e, 0}$, according to what is observed in the experiment.

6.2 Calculating the ground state

To calculate the coupling between the states $(e, 0)$ and $(g, \pm p)$, as described in equation (35) in section 5.1, we need the corresponding wave functions, which we can approximately calculate from the stationary GPE when we neglect the non-condensate contributions. In terms of the single-particle wave function $\phi(\mathbf{r})$ the stationary GPE (introduced in section 1.3) reads

$$\left(-\frac{\hbar^2}{2m} \nabla^2 + V_{\text{trap}}(\mathbf{r}) + gN|\phi(\mathbf{r})|^2 \right) \phi(\mathbf{r}) = \mu\phi(\mathbf{r}), \quad (36)$$

since $\Psi_0(\mathbf{r}) = \sqrt{N}\phi(\mathbf{r})$, with N being the number of particles in the condensate. Assuming $V_{\text{trap}}(\mathbf{r}) = V_x(x) + V_y(y) + V_z(z)$ for the confinement potential and approximating the wave function by the factorization $\phi(\mathbf{r}) = \phi_x(x)\phi_y(y)\phi_z(z)$ we obtain three coupled equations, from which those for $\phi_y(y)$ and $\phi_z(z)$ are solved in the approximation of no interaction, what is justified due to the high anisotropy of the trap. Using the ground states in y - and z -direction we can

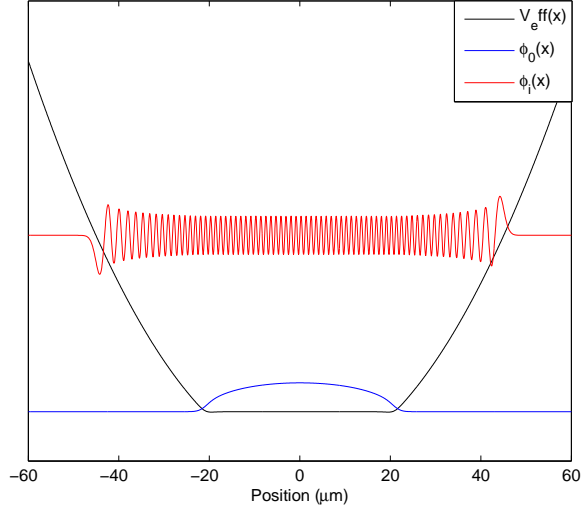


Figure 9: Effective potential in x -direction (black) with the longitudinal ground ϕ_0 (blue) and one particular, longitudinal excited twin-beam state ϕ_i (red).

write for the longitudinal direction

$$\left(-\frac{\hbar^2}{2m} \nabla_x^2 + V_x(x) + gN |\phi_x(x) \phi_y(y) \phi_z(z)|^2 \right) \phi_x(x) \phi_y(y) \phi_z(z) = \mu \phi_x(x) \phi_y(y) \phi_z(z), \quad (37)$$

which, multiplied by $\phi_y^*(y) \phi_z^*(z)$ and integrated with respect to y and z , gives

$$\left(-\frac{\hbar^2}{2m} \nabla_x^2 + V_x(x) + N\kappa |\phi_x(x)|^2 \right) \phi_x(x) = \mu \phi_x(x) \quad (38)$$

where $\kappa = g \int dy |\phi_y(y)|^4 \int dz |\phi_z(z)|^4$ is the one-dimensional interaction parameter, depending on the 3D interaction parameter g . The single-particle wave functions $\phi_y(y)$ and $\phi_z(z)$ are the ground state solutions in y - and z -direction. Hence, $\phi_x(x)$ satisfies a non-linear Schrödinger equation with the Hamiltonian

$$\hat{H}_x = -\frac{1}{2} \nabla_x^2 + V_x(x) + N\kappa |\phi_x(x)|^2 \quad (39)$$

from which the longitudinal ground state can be calculated self-consistently by employing imaginary time propagation (see figure 9). This leads to an effective potential in x -direction for which also the wave functions of the excited states can be calculated which will be used in the multi-mode description in section 6.6 to compute the coupling matrix elements κ_{ij} as well as the energies of the corresponding modes $E_{g,i}$.

6.3 Two-mode model

6.3.1 The Hamiltonian

As already mentioned in the introduction of this chapter, a simple model for the generation of twin-atom beams has to include the mode $(g, 0)$ which is the longitudinal and radial ground state of the trap, the radial excited state $(e, 0)$, and the wing states which are the longitudinal excited modes that are in the radial ground $(g, \pm p)$ and excited $(e, \pm p)$ state. This is sufficient to describe the excitation of the quasi-condensate from the (radial and longitudinal) ground state $(g, 0)$ of the trap to the state $(e, 0)$ by shaking of the condensate and the subsequent pairwise scattering of atoms from $(e, 0)$ to the longitudinal ground states $(g, \pm p)$.

Instead of describing the shaking of the condensate by a time-dependent confinement potential $V(y - y_0(t))$ a transformation to a frame moving with $y_0(t)$ is accomplished, leading to a static potential and an additional excitation term $-\wp\dot{y}_0$ where \wp is the momentum operator.

Using the formalism introduced in the previous chapter 5.1, we obtain the Hamiltonian

$$\hat{H}_0 = \sum_{k=0, \pm p} \left[\sum_{i=e, g} E_{i, k} \hat{a}_{i, k}^\dagger \hat{a}_{i, k} - \wp_{eg} \dot{y}_0 \left(\hat{a}_{e, k}^\dagger \hat{a}_{g, k} + \hat{a}_{g, k}^\dagger \hat{a}_{e, k} \right) \right], \quad (40)$$

which governs the single-particle dynamics, with $\wp_{eg} = \wp_{ge}$ being the momentum matrix element between the states $(e, 0)$ and $(g, 0)$. For the Hamiltonian, describing the atom-atom interaction we get

$$\hat{H}' = \kappa \left(\hat{a}_{g, p}^\dagger \hat{a}_{g, -p}^\dagger \hat{a}_{e, 0} \hat{a}_{e, 0} + \hat{a}_{e, 0}^\dagger \hat{a}_{e, 0}^\dagger \hat{a}_{g, p} \hat{a}_{g, -p} \right) \quad (41)$$

where

$$\kappa = g \int \phi_e^*(x)^2 \phi_g(x)^2 dx \int \phi_g^*(y)^2 \phi_e(y)^2 dy \int |\phi_g(z)|^4 dz \quad (42)$$

is the product of the coupling constant g and the wave function overlap matrix elements, cf. (35). Here the ϕ_g and ϕ_e are the single-particle states in longitudinal (x) and radial (y and z) direction for the ground (g) and excited (e) modes obtained as described in section 6.2. For simplicity, all other terms resulting from atom-atom interactions have been neglected because we are just interested in the contributions due to the atom-pair production.

6.3.2 Full solution of the Schrödinger equation

The resulting problem for the emission process in the real two-mode model can be accomplished by a numerical solution of the full Schrödinger equation. This allows the validation of the density matrix approach we will make in section 6.3.3. Therefore, in the following we solely consider the emission pro-

cess, i.e. the generation of atom pairs, due to scattering processes in the excited quasi-condensate, which can be described by the non-linear Hamiltonian $\hat{H}' = \kappa \hat{a}_{g,p}^\dagger \hat{a}_{g,p}^\dagger \hat{a}_{e,0} \hat{a}_{e,0} + \kappa \hat{a}_{e,0}^\dagger \hat{a}_{e,0}^\dagger \hat{a}_{g,p} \hat{a}_{g,p}$.

In general, the many-body wave function of a system of N identical bosons occupying M orbitals $\{\phi_1, \dots, \phi_M\}$ can be written as

$$|\Psi\rangle = \sum_{\vec{n}} C_{\vec{n}} |n_1, n_2, \dots, n_M\rangle, \quad (43)$$

where the vector \vec{n} contains the occupation numbers of the single orbitals $\vec{n} = (n_1, n_2, \dots, n_M)$ with $n_1 + n_2 + \dots + n_M = N$ and the sum running over all possible configurations [29].

Hence, to model the emission process, we use the many-body wave function

$$|\Psi\rangle = \sum_{m=0}^N C_m |n_0 = N - m, n_p = m\rangle, \quad (44)$$

where n_0 is the number of particles in the excited state $(e, 0)$ and n_p is the sum of particles in the modes $(g, +p)$ and $(g, -p)$. (Due to the Hamiltonian \hat{H}' , which allows only for the annihilation and creation of atom pairs, the coefficients C_m vanish, when m is odd.)

Applying the Hamiltonian \hat{H}' on a certain configuration $|n_0, n_p\rangle$ yields

$$\begin{aligned} \hat{H}' |n_0, n_p\rangle = & \kappa \sqrt{(n_p + 1)(n_p + 2)} \sqrt{n_0(n_0 - 1)} |n_0 - 2, n_p + 1\rangle + \\ & \kappa \sqrt{(n_0 + 1)(n_0 + 2)} \sqrt{n_p(n_p - 1)} |n_0 + 2, n_p - 1\rangle. \end{aligned} \quad (45)$$

In an analogous manner we can calculate the expectation values of the one- and two-particle density matrices, what gives

$$\rho_{ee,0} = \langle \hat{a}_{e,0}^\dagger \hat{a}_{e,0} \rangle = \langle \Psi | \hat{a}_{e,0}^\dagger \hat{a}_{e,0} | \Psi \rangle = \sum_{m=0}^N (N - m) |C_m|^2 \quad (46)$$

$$\rho_{gg,p} = \langle \Psi | \hat{a}_{g,p}^\dagger \hat{a}_{g,p} | \Psi \rangle = \sum_{m=0}^N m |C_m|^2 \quad (47)$$

and

$$\langle \hat{a}_{e,0}^\dagger \hat{a}_{e,0}^\dagger \hat{a}_{e,0} \hat{a}_{e,0} \rangle = \langle \hat{a}_{e,0}^\dagger \hat{a}_{e,0} \hat{a}_{e,0}^\dagger \hat{a}_{e,0} \rangle - \rho_{ee,0} = \sum_{m=0}^N (N - m)^2 |C_m|^2 - \rho_{ee,0} \quad (48)$$

$$\langle \hat{a}_{g,p}^\dagger \hat{a}_{g,p}^\dagger \hat{a}_{g,p} \hat{a}_{g,p} \rangle = \langle \hat{a}_{g,p}^\dagger \hat{a}_{g,p} \hat{a}_{g,p}^\dagger \hat{a}_{g,p} \rangle - \rho_{gg,p} = \sum_{m=0}^N m^2 |C_m|^2 - \rho_{gg,p} \quad (49)$$

For the simulation we start with the quasi-condensate being entirely in the $(e, 0)$ state, and hence, with the total wave-function being $|\Psi\rangle = |n_0 = N, n_p = 0\rangle$ and approximate the coupling constant through $\kappa = 1/n$. We calculate the time-evolution of the wave-function by solving the Schrödinger equation, using the Crank-Nicolson method. The results are shown in figure 10.

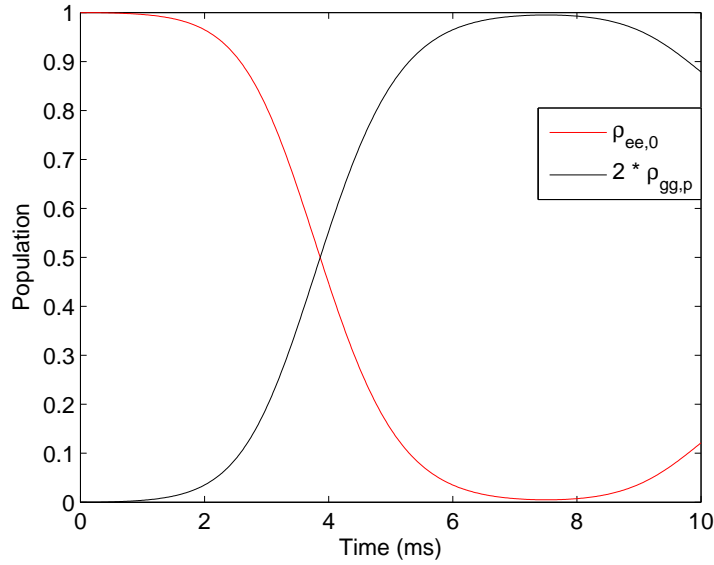


Figure 10: Occupation density of the states $(e, 0)$ and $(g, \pm p)$ for the exact solvable two-mode model of the emission process

6.3.3 Density matrix approach

Alternatively we could consider the time evolution of the operators $\hat{a}_{i,k}$, or better examine that of the direct observable quantities $\langle \hat{a}_{i,k}^\dagger \hat{a}_{j,k} \rangle$ what we will do in the following. The expectation values define the single-particle density matrices $\rho_{ij,k} = \langle \hat{a}_{i,k}^\dagger \hat{a}_{j,k} \rangle$, with their time evolution given by the Heisenberg equations of motion $i\dot{\rho}_{ij,k} = \langle [\hat{a}_{i,k}^\dagger \hat{a}_{j,k}, \hat{H}_0 + \hat{H}'] \rangle$. Through \hat{H}' the time evolution of the expectation values of the single-particle density matrices do also depend on the two-particle density matrices $\Delta_{ij,kl} = \langle \hat{a}_{i,p}^\dagger \hat{a}_{j,-p}^\dagger \hat{a}_{k,0} \hat{a}_{l,0} \rangle$ which accounts for the correlation, induced by scattering processes where two atoms in $(e, 0)$ are scattered to the final states (g, p) and $(g, -p)$.

Setting up the Heisenberg equations of motion for the one-particle density matrices, we get

$$i\dot{\rho}_{ee,0} = -i\wp_{eg}\dot{y}_0 2 \text{Im} \rho_{eg,0} - 4i\kappa \text{Im} \Delta_{gg,ee} \quad (50a)$$

$$i\dot{\rho}_{gg,p} = i\wp_{eg}\dot{y}_0 2 \text{Im} \rho_{eg,p} + 2i\kappa \text{Im} \Delta_{gg,ee}. \quad (50b)$$

Similarly we obtain the Heisenberg equation of motions for the two-particle density matrices, which through \hat{H}' couple to a three-particle density matrix, what is in accordance to the BBGKY hierarchy of interacting many particle systems (see 5.2). So we see, e.g., from the time evolution of the two-particle

density matrix $\Delta_{gg,ee}$

$$\begin{aligned} i\dot{\Delta}'_{gg,ee} &= \left\langle \left[\hat{a}_{g,p}^\dagger \hat{a}_{g,-p}^\dagger \hat{a}_{e,0} \hat{a}_{e,0}, \hat{H}' \right] \right\rangle = \\ &= 2\kappa \left\langle \hat{a}_{g,p}^\dagger \hat{a}_{g,-p}^\dagger \left(\hat{a}_{e,0}^\dagger \hat{a}_{g,p} \hat{a}_{g,-p} \hat{a}_{e,0} + \hat{a}_{e,0} \hat{a}_{e,0}^\dagger \hat{a}_{g,p} \hat{a}_{g,-p} \right) \right\rangle + \\ &\quad - \kappa \left\langle \left(\hat{a}_{g,-p} \hat{a}_{g,-p}^\dagger + \hat{a}_{g,p}^\dagger \hat{a}_{g,p} \right) \hat{a}_{e,0}^\dagger \hat{a}_{e,0} \hat{a}_{e,0} \hat{a}_{e,0} \right\rangle, \end{aligned} \quad (51)$$

the dependence on the three-particle density matrices. In order to obtain a closed set of equations of motions this hierarchy has to be truncated.

First-order approximation

In lowest-order, the three-particle density matrices can be approximated by products of two-particle density matrices, which in the case of the three-particle density matrix $\langle \hat{a}_{g,p}^\dagger \hat{a}_{g,-p}^\dagger \hat{a}_{e,0}^\dagger \hat{a}_{g,p} \hat{a}_{g,-p} \hat{a}_{e,0} \rangle$ arising in (51) takes the form

$$\begin{aligned} \langle \hat{a}_{g,p}^\dagger \hat{a}_{g,-p}^\dagger \hat{a}_{e,0}^\dagger \hat{a}_{g,p} \hat{a}_{g,-p} \hat{a}_{e,0} \rangle &\simeq \langle \hat{a}_{g,p}^\dagger \hat{a}_{g,p} \rangle \langle \hat{a}_{g,-p}^\dagger \hat{a}_{g,-p} \rangle \langle \hat{a}_{e,0}^\dagger \hat{a}_{e,0} \rangle \\ &= \rho_{gg,p}^2 \rho_{ee,0}. \end{aligned} \quad (52)$$

Applying this truncation scheme to the equation of motion for the two-particle density matrix $\Delta_{gg,ee}$ we obtain

$$i\dot{\Delta}'_{gg,ee} \simeq 2\kappa \rho_{gg,p}^2 (2\rho_{ee,0} + 1) - \kappa (2\rho_{gg,p} + 1) \rho_{ee,0} (\rho_{ee,0} - 1) \quad (53)$$

due to \hat{H}' and the terms resulting from \hat{H}_0 can be derived in complete analogy to (50), what gives

$$\begin{aligned} i\dot{\Delta}^0_{gg,ee} &= \left\langle \left[\hat{a}_{g,p}^\dagger \hat{a}_{g,-p}^\dagger \hat{a}_{e,0} \hat{a}_{e,0}, \hat{H}_0 \right] \right\rangle = \\ &= 2\Delta_{gg,ee} (E_{e,0} - E_{g,p}) - 2\wp_{eg} \dot{y}_0 (\Delta_{gg,eg} - \Delta_{eg,ee}). \end{aligned} \quad (54)$$

Analogously all further equations for the time evolution of the one- and two-particle density matrices can be calculated. The complete set of equations is listed in appendix A.1.1. This closed set of equations can be solved in parallel, the results are shown in figure 11. For the simulation a coupling constant of $\kappa = 1/n$ and the initial conditions

$$\begin{aligned} \rho_{ee,0} &= 0 \\ \rho_{gg,p} &= N \end{aligned} \quad (55)$$

$$\Delta_{gg,ee} = 0 \quad (56)$$

have been used. Where $N = 700$ is the total number of particles. For the energies the experimental values of $E_{g,0} = h \cdot 1.83$, $E_{e,0} = E_{g,\pm p} = h \cdot 2.58$ and $E_{e,\pm p} = h \cdot 5.16$ are used. The trajectory of the potential minimum for the transverse shaking of the trap for the first 5 ms of excitation is described by $V(y) = V(y - 0.022 \sin(E_{e,0}t))$ and the momentum matrix element is set as $\wp_{eg} = -2.45$.

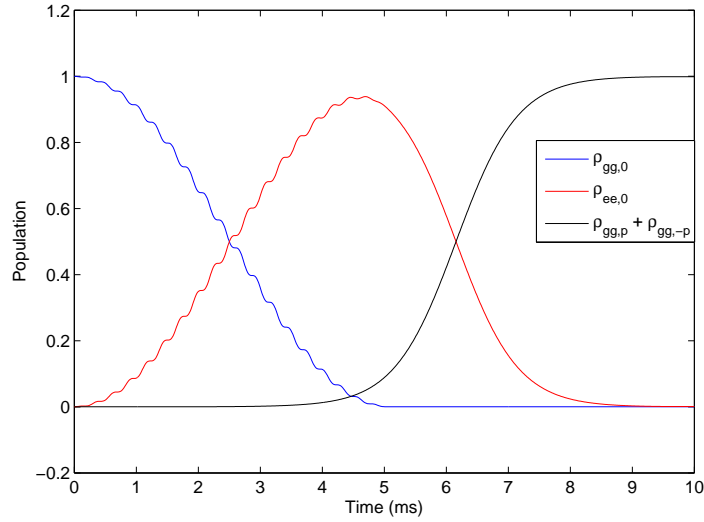


Figure 11: Populations of the ground and excited states with zero and finite momenta, while shaking up the condensate with $V(y - 0.02 \sin(E_{e,0}t))$ in the first 5 ms and subsequent emission of atom pairs into the longitudinal modes.

Comparison

In figure 12 we compare the exact results for the emission process from section 6.3.2, which result from the numerical solution of the full Schrödinger equation, to those described in the last paragraph, obtained from the density matrix approach and the approximation of the three-particle density matrices by products of one-particle density matrices, i.e. $\langle ABC \rangle \simeq \langle A \rangle \langle B \rangle \langle C \rangle$.

Since in this approximation, we have neglected all coupling terms between one- and two-particle density matrices we will truncate the hierarchy of equations of motion at one level deeper and see if we can get better agreement with the exact solution. This is the topic of the next paragraph.

Second-order approximation

In the following we will also include the coupling terms between one- and two-particle density matrices. The three-particle density matrices are then approximated by $\langle ABC \rangle \simeq \langle AB \rangle \langle C \rangle + \langle A \rangle \langle BC \rangle + \langle AC \rangle \langle B \rangle - 2\langle A \rangle \langle B \rangle \langle C \rangle$. For the equation of motion for the two-particle density matrix $\Delta_{gg,ee}$, we hence

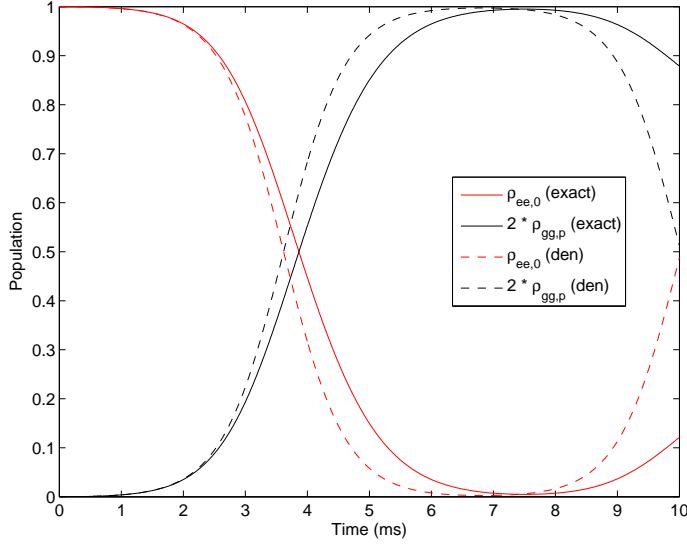


Figure 12: Comparison of the population of the states $(e, 0)$ and $(g, \pm p)$ of the two-mode model of the emission process for the exact solvable (solid line) and the density matrix approach with the truncation scheme $\langle ABC \rangle \simeq \langle A \rangle \langle B \rangle \langle C \rangle$ (dashed line).

get

$$\begin{aligned}
 i\dot{\Delta}_{gg,ee} = & \langle [\hat{a}_{g,p}^\dagger \hat{a}_{g,-p}^\dagger \hat{a}_{e,0} \hat{a}_{e,0}, \hat{H}'] \rangle \simeq 4\kappa \langle \hat{a}_{g,p}^\dagger \hat{a}_{g,-p}^\dagger \hat{a}_{g,p} \hat{a}_{g,-p} \rangle \langle \hat{a}_{e,0}^\dagger \hat{a}_{e,0} \rangle + \\
 & + 8\kappa \langle \hat{a}_{g,p}^\dagger \hat{a}_{g,p} \rangle \langle \hat{a}_{g,p}^\dagger \hat{a}_{e,0}^\dagger \hat{a}_{g,p} \hat{a}_{e,0} \rangle - 8\kappa \langle \hat{a}_{g,p}^\dagger \hat{a}_{g,p} \rangle^2 \langle \hat{a}_{e,0}^\dagger \hat{a}_{e,0} \rangle + \\
 & + 2\kappa \langle \hat{a}_{g,p}^\dagger \hat{a}_{g,-p}^\dagger \hat{a}_{g,p} \hat{a}_{g,-p} \rangle - 4\kappa \langle \hat{a}_{e,0}^\dagger \hat{a}_{g,p}^\dagger \hat{a}_{e,0} \hat{a}_{g,p} \rangle \langle \hat{a}_{e,0}^\dagger \hat{a}_{e,0} \rangle + \\
 & - 2\kappa \langle \hat{a}_{g,p}^\dagger \hat{a}_{g,p} \rangle \langle \hat{a}_{e,0}^\dagger \hat{a}_{e,0}^\dagger \hat{a}_{e,0} \hat{a}_{e,0} \rangle + 4\kappa \langle \hat{a}_{g,p}^\dagger \hat{a}_{g,p} \rangle \langle \hat{a}_{e,0}^\dagger \hat{a}_{e,0} \rangle^2 + \\
 & - \kappa \langle \hat{a}_{e,0}^\dagger \hat{a}_{e,0}^\dagger \hat{a}_{e,0} \hat{a}_{e,0} \rangle. \tag{57}
 \end{aligned}$$

The equations of motion for the other two-particle density matrices involved are calculated in the same way and the results are listed in appendix A.1.2. The equations of motion for the one-particle density matrices are not affected by this new factorization scheme and remain the same as in equation (50). If we solve the occurring system of coupled differential equations we still see the inconsistency between the exact solution of the Schrödinger equation and that obtained from the density matrix approaches, that already occur at early times (see figure 13). For later times the new factorization gives an even worse approximation. To find out why this is the case, we will, in section 6.4, compare our results to those obtained by Anglin and Vardi in [30, 31] for the problem of a two-mode model of a condensate in a double well trap.

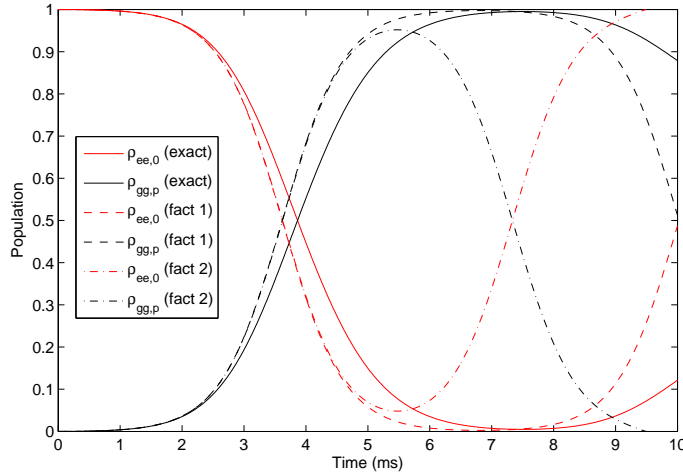


Figure 13: Occupation density of the states $(e, 0)$ and $(g, \pm p)$ of the emission process for the exact solvable two-mode model (solid line) and the density matrix approach applying the truncation scheme $\langle ABC \rangle \simeq \langle AB \rangle \langle C \rangle + \langle A \rangle \langle BC \rangle + \langle AC \rangle \langle B \rangle - 2\langle A \rangle \langle B \rangle \langle C \rangle$ (dashed line).

6.3.4 Pseudospin-operator approach

In the following section we apply the approach developed by Anglin and Vardi to calculate the dynamics of a condensate in a double-well trap, that is mapped onto a two-mode model [30, 31] to the generation of twin-atom beams. Within this approach, not the evolution of the expectation values $\langle \hat{a}_i^\dagger \hat{a}_j \rangle$ is calculated, but that of the angular momentum operators in the Bloch representation which are defined as

$$\hat{L}_x \equiv \frac{\hat{a}_{e,0}^\dagger \hat{a}_{g,p} + \hat{a}_{g,p}^\dagger \hat{a}_{e,0}}{2} \quad (58a)$$

$$\hat{L}_y \equiv \frac{\hat{a}_{e,0}^\dagger \hat{a}_{g,p} - \hat{a}_{g,p}^\dagger \hat{a}_{e,0}}{2i} \quad (58b)$$

$$\hat{L}_z \equiv \frac{\hat{a}_{e,0}^\dagger \hat{a}_{e,0} - \hat{a}_{g,p}^\dagger \hat{a}_{g,p}}{2} \quad (58c)$$

and

$$\hat{L}_+ \equiv \hat{L}_x + i\hat{L}_y = \hat{a}_{e,0}^\dagger \hat{a}_{g,p} \quad \hat{L}_- \equiv \hat{L}_x - i\hat{L}_y = \hat{a}_{g,p}^\dagger \hat{a}_{e,0} \quad (59)$$

are the coresponding ladder operators. In terms of these $SU(2)$ generators the two-mode Hamiltonian reads

$$\begin{aligned} \hat{H}' &= \frac{\kappa}{2} \left(\hat{a}_{g,p}^\dagger \hat{a}_{g,p}^\dagger \hat{a}_{e,0} \hat{a}_{e,0} + \hat{a}_{e,0}^\dagger \hat{a}_{e,0}^\dagger \hat{a}_{g,p} \hat{a}_{g,p} \right) \\ &= \frac{\kappa}{2} \left(\hat{L}_-^2 + \hat{L}_+^2 \right) = \kappa \left(\hat{L}_x^2 - \hat{L}_y^2 \right). \end{aligned} \quad (60)$$

We are especially interested in the value of the operator \hat{L}_z because it represents the number difference of atoms in the excited state $(e, 0)$ and that of atoms in

the wing-states ($g, \pm p$). So we calculate the corresponding Heisenberg equations of motion for this angular momentum operator giving

$$\frac{d}{dt}\hat{L}_z = -i[\hat{L}_z, \hat{H}'] = 2\kappa(\hat{L}_x\hat{L}_y + \hat{L}_y\hat{L}_x). \quad (61)$$

Again, the expectation values $\langle\hat{L}_i\hat{L}_j\rangle$ can, in lowest order, be approximated by the product of first order expectation values by $\langle\hat{L}_i\hat{L}_j\rangle \approx \langle\hat{L}_i\rangle\langle\hat{L}_j\rangle$. Here this approximation is insufficient, since if all the atoms are initially in the excited state ($e, 0$) only the expectation value $\langle\hat{L}_z\rangle$ is different from zero in the beginning, and time derivation of all three angular momentum operators vanishes. This is why we have to go one level deeper and instead also consider the time evolution of the second order moments and apply the approximation

$$\langle\hat{L}_i\hat{L}_j\hat{L}_k\rangle \approx \langle\hat{L}_i\hat{L}_j\rangle\langle\hat{L}_k\rangle + \langle\hat{L}_i\rangle\langle\hat{L}_j\hat{L}_k\rangle + \langle\hat{L}_i\hat{L}_k\rangle\langle\hat{L}_j\rangle - 2\langle\hat{L}_i\rangle\langle\hat{L}_j\rangle\langle\hat{L}_k\rangle. \quad (62)$$

Implementing this truncation we get for the time evolution of the second order moment $\langle\hat{L}_x\hat{L}_y\rangle$

$$\begin{aligned} \frac{d}{dt}\langle\hat{L}_x\hat{L}_y\rangle &\simeq \\ &\simeq -6\kappa\langle\hat{L}_x\rangle\langle\hat{L}_x\hat{L}_z\rangle - 4\kappa\langle\hat{L}_z\rangle\langle\hat{L}_x\hat{L}_x\rangle - 2\kappa\langle\hat{L}_x\rangle\langle\hat{L}_z\hat{L}_x\rangle + 8\kappa\langle\hat{L}_x\rangle\langle\hat{L}_x\rangle\langle\hat{L}_z\rangle + \\ &\quad - 6\kappa\langle\hat{L}_y\rangle\langle\hat{L}_z\hat{L}_y\rangle - 4\kappa\langle\hat{L}_z\rangle\langle\hat{L}_y\hat{L}_y\rangle - 2\kappa\langle\hat{L}_y\hat{L}_z\rangle\langle\hat{L}_y\rangle + 8\kappa\langle\hat{L}_y\rangle\langle\hat{L}_y\rangle\langle\hat{L}_z\rangle. \end{aligned} \quad (63)$$

and derive the remaining equations analogously. Here we see that we also need the time evolution for the operators \hat{L}_x and \hat{L}_y , which are calculated like that for \hat{L}_z in (61). The whole system of equations of motions is listed in appendix A.1.3. We solve these equations in parallel, analogously to those in section 6.3.3. From these results we can calculate the population of the excited ($e, 0$) and wing states ($g, \pm p$) by

$$N_p = \frac{N}{2} - \langle\hat{L}_z\rangle \quad (64)$$

since

$$\langle\hat{L}_z\rangle = \frac{N_0 - N_p}{2} \quad \text{and} \quad N = N_0 + N_p \quad (65)$$

where N is the total number of particles. In figure 14 we show the corresponding plot. The comparison with the results from section 6.3.3 and the plot in figure 12 respectively, shows accordance to a large extent what means that the truncation scheme $\langle ABC \rangle \simeq \langle A \rangle \langle B \rangle \langle C \rangle$ applied in 6.3.3 is as good as the approximation applied within the pseudospin-operator approach in equation (62).

For a more intuitive understanding for the phase and particle number fluctuations we define the single-particle Bloch vector

$$\vec{S} \equiv (S_x, S_y, S_z) = \left(\frac{2\langle\hat{L}_x\rangle}{N}, \frac{2\langle\hat{L}_y\rangle}{N}, \frac{2\langle\hat{L}_z\rangle}{N} \right) \quad (66)$$

and visualize the dynamics on a Bloch sphere.

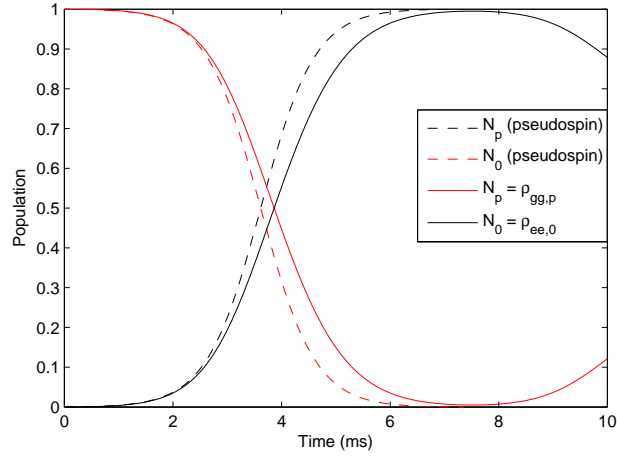


Figure 14: Occupation density of the states $(e, 0)$ and $(g, \pm p)$ of the emission process for the exact solvable two-mode model vs. the pseudospin-operator approach.



Figure 15: The generation of twin-atom beams visualized on the Bloch sphere with time increasing from left to right.

Visualization on the Bloch sphere

For a two-mode N -particle system we can apply the principles for the visualization of an assembly of two-level atoms in quantum optics from [32]. An atomic coherent state $|\theta, \phi\rangle$ is obtained by rotations of the ground state which, in the case of the two-mode model, we chose to be the $|N, 0\rangle$ where all atoms are in the excited state $(e, 0)$, what can be written as

$$|\theta, \phi\rangle = R_{\theta, \phi}|N, 0\rangle \quad (67)$$

where the rotation matrix is given by $R_{\theta, \phi} = e^{-i\theta(\hat{J}_x \sin \phi - \hat{J}_y \cos \phi)}$. The probability distribution for the states $|C\rangle$ obtained by the time-evolution corresponding to \hat{H}' is given by $|\langle \theta, \phi | C \rangle|^2$ what is illustrated in figure 15 where the number difference is plotted on the z -axis and the phase on the y -axis. For the twin-atom beam generation, one can furthermore see that the number and density fluctuations (which are represented by the widths in z - and y -direction) increase and subsequently decrease again.

6.4 Truncation of the hierarchy of expectation value equations of motion

In equation (57) we applied a truncation scheme on the hierarchy of equations of motion for the density matrices, from which we expected to obtain better agreement with the exact solution of the full Schrödinger equation but that was not the case (see figure 13). Namely we have factorized the three-particle density matrix elements like $\langle ABC \rangle \simeq \langle AB \rangle \langle C \rangle + \langle A \rangle \langle BC \rangle + \langle AC \rangle \langle B \rangle - 2\langle A \rangle \langle B \rangle \langle C \rangle$ instead of neglecting the coupling terms between one- and two-particle density matrices and factorizing the three-particle density matrix as $\langle ABC \rangle \simeq \langle A \rangle \langle B \rangle \langle C \rangle$ which is applied in equation (53). To understand why this new factorization does not give a better approximation we compare our results to those obtained by Anglin and Vardi [30, 31] for the two-mode model realized by a condensate in a double well trap. In the following section which we will shortly retrace the corresponding calculations.

6.4.1 Two-mode model of a condensate in a double well trap

For the condensate in a double well trap we have two modes which we will call left and right mode. If $\hat{a}_{L,R}^\dagger$ and $\hat{a}_{L,R}$ are the creation and annihilation operators for the corresponding modes, we can define the angular momentum operators as

$$\hat{L}_x \equiv \frac{\hat{a}_L^\dagger \hat{a}_R + \hat{a}_R^\dagger \hat{a}_L}{2} \quad (68a)$$

$$\hat{L}_y \equiv \frac{\hat{a}_L^\dagger \hat{a}_R - \hat{a}_R^\dagger \hat{a}_L}{2i} \quad (68b)$$

$$\hat{L}_z \equiv \frac{\hat{a}_L^\dagger \hat{a}_L - \hat{a}_R^\dagger \hat{a}_R}{2}. \quad (68c)$$

In terms of these angular momentum operators the Hamiltonian, describing a condensate in a double well trap, takes the form

$$\hat{H} = -\omega \hat{L}_x + \frac{\eta}{2} \hat{L}_z^2 \quad (69)$$

where ω labels the tunnel coupling and η the interaction strength between the two modes.

Like in section 6.3.3 the equations of motion for the expectation values of the angular momentum operators can be calculated from $\frac{d}{dt} \langle \hat{L}_i \rangle = -i \langle [\hat{L}_i, \hat{H}] \rangle$ and depend on the second order moments $\Delta_{ij} \equiv \langle \hat{L}_i \hat{L}_j + \hat{L}_j \hat{L}_i \rangle - 2\langle \hat{L}_i \rangle \langle \hat{L}_j \rangle$. Due to the BBGKY hierarchy the second order moments depend on third order moments. This is the point where we apply the different factorizations $\langle \hat{L}_i \hat{L}_j \hat{L}_k \rangle \simeq \langle \hat{L}_i \rangle \langle \hat{L}_j \rangle \langle \hat{L}_k \rangle$ and $\langle \hat{L}_i \hat{L}_j \hat{L}_k \rangle \simeq \langle \hat{L}_i \hat{L}_j \rangle \langle \hat{L}_k \rangle + \langle \hat{L}_i \rangle \langle \hat{L}_j \hat{L}_k \rangle + \langle \hat{L}_i \hat{L}_k \rangle \langle \hat{L}_j \rangle - 2\langle \hat{L}_i \rangle \langle \hat{L}_j \rangle \langle \hat{L}_k \rangle$. Based on the resulting sets of equations of motion for the first and second order expectation values we can run simulations (see

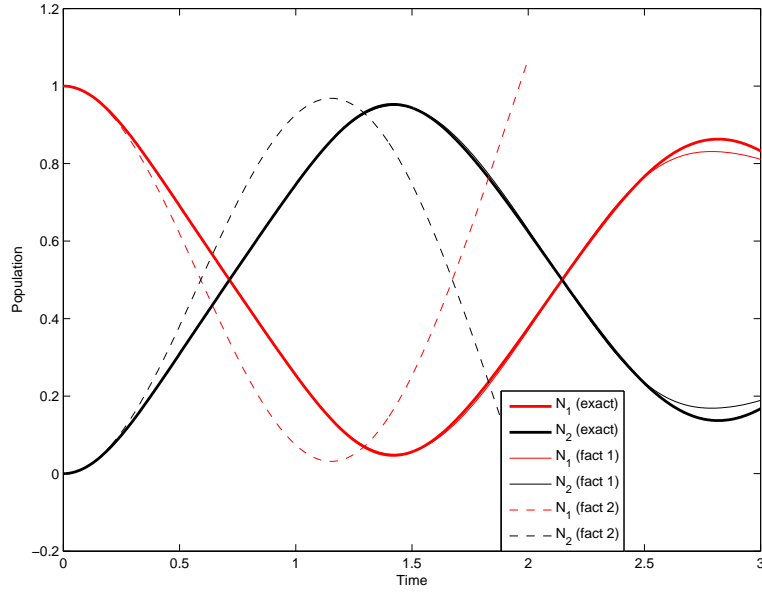


Figure 16: Comparison between the two factorization schemes $\langle \hat{L}_i \hat{L}_j \hat{L}_k \rangle \simeq \langle \hat{L}_i \rangle \langle \hat{L}_j \rangle \langle \hat{L}_k \rangle$ (fact 2) and $\langle \hat{L}_i \hat{L}_j \hat{L}_k \rangle \simeq \langle \hat{L}_i \hat{L}_j \rangle \langle \hat{L}_k \rangle + \langle \hat{L}_i \rangle \langle \hat{L}_j \hat{L}_k \rangle + \langle \hat{L}_i \hat{L}_k \rangle \langle \hat{L}_j \rangle - 2 \langle \hat{L}_i \rangle \langle \hat{L}_j \rangle \langle \hat{L}_k \rangle$ (fact 1) against the exact solution of the Schrödinger equation (exact) for a condensate in a double well.

figure 16, similar to those already used for the calculation of the twin-atom beam generation. Here we start with the condensate being initially entirely in the left mode what is implemented by the use of the following initial conditions

$$\begin{aligned}
 \langle \hat{L}_z \rangle &= \frac{N}{2} \\
 \Delta_{xx} &= \Delta_{yy} = \frac{N}{2} \\
 \langle \hat{L}_x \rangle &= \langle \hat{L}_y \rangle = \Delta_{xy} = \Delta_{xz} = \Delta_{yz} = \Delta_{zz} = 0.
 \end{aligned} \tag{70}$$

6.4.2 Comparison of the two-mode models of a condensate in double well versus that of twin-atom beam generation

In figure 16 we compare the results obtained by the two different factorization schemes, and see much better agreement of the factorization which includes the coupling between first and second order moments to the exact solution. This is what we have also expected for the simulation of the generation of twin-atom beams, but there we obtained better results with the application of the factorization $\langle ABC \rangle \simeq \langle A \rangle \langle B \rangle \langle C \rangle$ as shown in figure 13. This may be the case since the

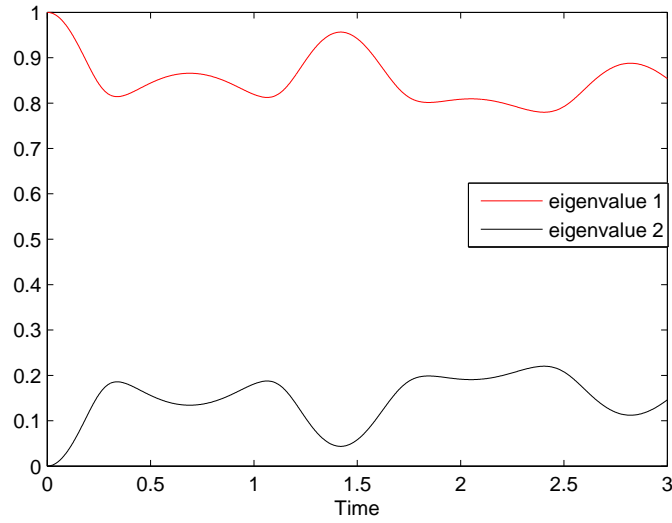


Figure 17: Eigenvalues of the RSPDM for a condensate in a double well.

factorization $\langle \hat{L}_i \hat{L}_j \hat{L}_k \rangle \simeq \langle \hat{L}_i \hat{L}_j \rangle \langle \hat{L}_k \rangle + \langle \hat{L}_i \rangle \langle \hat{L}_j \hat{L}_k \rangle + \langle \hat{L}_i \hat{L}_k \rangle \langle \hat{L}_j \rangle - 2 \langle \hat{L}_i \rangle \langle \hat{L}_j \rangle \langle \hat{L}_k \rangle$ is a perturbative approximation in f , where f and $1 - f$ are the eigenvalues of the reduced single particle density matrix (RSPDM) with the elements $R_{ij} = \langle \hat{a}_i^\dagger \hat{a}_j \rangle / N$ and therefore only valid if f is small, what is related to mildly fragmented condensate [30]. For the problem of a condensate in a double well this condition is fulfilled as we can easily check by plotting the eigenvalues of the RSPDM (see figure 17) but it is not the case for the problem of twin-atom beam generation, where the first eigenvalue of the RSPDM equals the population of the excited state ($e, 0$) and the second one that of the wing state ($g, \pm p$).

6.5 Coupled-cluster approximation

In the previous chapters we have probed different truncation schemes within the density-matrix approach and obtained a good approximation, already close to the exact result (see figure 12). Nevertheless, in the following section, we want to apply a different approach, namely the coupled-cluster theory, to see if we can get even better results.

6.5.1 Basics of the coupled-cluster theory

Coupled-cluster theory was first suggested in the context of the many-body problem of nuclear physics by Coester [33] and Coester and Kümmel [34] and applied to a system of bosons in external traps by Cederbaum *et al* [35]. Within

the coupled-cluster approach the full many-body wave function is obtained from a ground configuration $|\phi_0\rangle$ by the application of an exponential operator $\exp(\hat{T})$

$$|\Psi\rangle = e^{\hat{T}}|\phi_0\rangle. \quad (71)$$

Whereas in the case of nuclear dynamics the ground configuration $|\phi_0\rangle$ is a Slater determinant, we will focus in the following on the system of N bosons, where the ground configuration naturally is given by the state where all particles remain in a single orbital φ_1 . This state can be written as

$$|\phi_0\rangle = \frac{1}{\sqrt{N!}} (\hat{a}_1^\dagger)^N |0\rangle \quad \text{with} \quad \langle\phi_0|\phi_0\rangle = 1 \quad (72)$$

where $|0\rangle$ is the vacuum state and \hat{a}_1^\dagger the creation operator corresponding to the orbital φ_1 . The *cluster operator* \hat{T} is defined as the sum of excitation operators \hat{T}_i

$$\hat{T} = \sum_{n=1}^N \hat{T}_n \quad (73)$$

where the excitation operator \hat{T}_1 generates a single excitation, \hat{T}_2 a double excitation and so on. These excitation operators can be written as

$$\hat{T}_n = \hat{t}_n (\hat{a}_1)^n \quad (74)$$

with

$$\hat{t}_n = \sum_{i_1, \dots, i_n=2}^M c_{i_1, \dots, i_n} \hat{a}_{i_1}^\dagger \cdots \hat{a}_{i_n}^\dagger \quad (75)$$

where m is the number of orbitals φ_i and the \hat{a}_i and \hat{a}_i^\dagger are the corresponding annihilation and creation operators. Since the creation operators in (75) commute, the order of the coefficients' indices is irrelevant. The *cluster amplitudes* c_{i_1, \dots, i_n} are yet unknown and can be calculated from the *coupled-cluster equations*. These coupled-cluster equations are obtained from the time-dependent Schrödinger equation

$$He^{\hat{T}}|\phi_0\rangle = i\frac{\partial}{\partial t}e^{\hat{T}}|\phi_0\rangle \quad (76)$$

which, multiplied with the operator $\exp(-\hat{T})$ from the left, gives

$$e^{-\hat{T}}He^{\hat{T}}|\phi_0\rangle = ie^{-\hat{T}}\frac{\partial}{\partial t}e^{\hat{T}}|\phi_0\rangle \quad (77)$$

and the projection onto the different possible excited configurations yields the following set of coupled equations

$$\langle \phi_0 | e^{-\hat{T}} H e^{\hat{T}} | \phi_0 \rangle = i \langle \phi_0 | e^{-\hat{T}} \frac{\partial}{\partial t} e^{\hat{T}} | \phi_0 \rangle \quad (78a)$$

$$\langle \phi_0 | \hat{a}_1^\dagger \hat{a}_i e^{-\hat{T}} H e^{\hat{T}} | \phi_0 \rangle = i \langle \phi_0 | \hat{a}_1^\dagger \hat{a}_i e^{-\hat{T}} \frac{\partial}{\partial t} e^{\hat{T}} | \phi_0 \rangle, \quad i = 2, 3, \dots, M \quad (78b)$$

$$\begin{aligned} \langle \phi_0 | \left(\hat{a}_1^\dagger \right)^2 \hat{a}_i \hat{a}_j e^{-\hat{T}} H e^{\hat{T}} | \phi_0 \rangle = \\ = i \langle \phi_0 | \left(\hat{a}_1^\dagger \right)^2 \hat{a}_i \hat{a}_j e^{-\hat{T}} \frac{\partial}{\partial t} e^{\hat{T}} | \phi_0 \rangle, \quad i \geq j = 2, 3, \dots, M \end{aligned} \quad (78c)$$

⋮

consisting of $\binom{M+N-1}{N}$ independent equations to calculate the $\binom{M+N-1}{N}$ cluster amplitudes c_{i_1, \dots, i_n} [35]. Since, even for a modest number of orbitals included, the size of this system of equations is enormous and an approximation becomes necessary.

The approximation is achieved by a truncation of the cluster operator \hat{T} . If, for example, the a CCSD approach is chosen, only single (S) and double (D) excitations operators are included, i.e. the cluster operator is approximated by $\hat{T} \approx \hat{T}_1 + \hat{T}_2$ and the number of cluster amplitudes reduces drastically to $M - 1$ coefficients c_i and $M(M - 1)/2$ coefficients c_{ij} (cf. (75)).

6.5.2 Application of coupled-cluster theory to the generation of twin-atom beams

In the last chapter we have reproduced the formalism of coupled-cluster theory for systems of bosons. In the following we apply this theory to the two-mode approximation of the generation of twin-atom beams out of an excited degenerate Bose gas. This process is described by the Hamiltonian

$$\hat{H}' = \kappa \left(\hat{a}_{g,p}^\dagger \hat{a}_{g,p}^\dagger \hat{a}_{e,0} \hat{a}_{e,0} + \hat{a}_{e,0}^\dagger \hat{a}_{e,0}^\dagger \hat{a}_{g,p} \hat{a}_{g,p} \right) \quad (79)$$

which we are already familiar to.

As in 6.5.1 we write the exact wave function as

$$|\Psi\rangle = e^{\hat{T}} |\phi_0\rangle \quad (80)$$

where here the ground configuration is chosen to be the state where all bosons are in the excited mode $(e, 0)$, which is

$$|\phi_0\rangle = \frac{1}{\sqrt{N!}} \left(\hat{a}_{e,0}^\dagger \right)^N |0\rangle \quad \text{with} \quad \langle \phi_0 | \phi_0 \rangle = 1. \quad (81)$$

Since in this system always pairs of atoms are generated in the longitudinal $(g, \pm p)$ modes, the cluster operator can only consist of double excitation operators or multiples of it. To demonstrate the underlying calculations we choose the following truncation of the cluster operator

$$\hat{T} = \hat{T}_2 + \hat{T}_4. \quad (82)$$

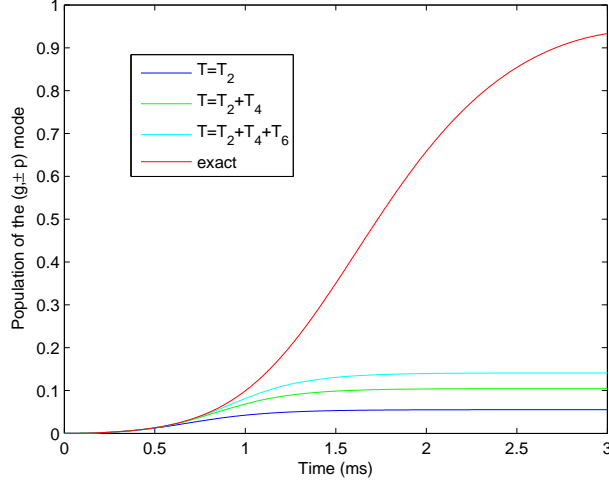


Figure 18: Occupation density of the wing states ($g, \pm p$) of the emission process for the exact solvable two-mode model and the two-mode coupled-cluster approach with different truncations of the cluster operator \hat{T} .

Since in our model we only have to deal with two modes, namely the $(e, 0)$ and $(g, \pm p)$ modes, here we simply label the occurring cluster amplitudes as t_2 and t_4 which, in our time-dependent problem are the quantities depending on time. So we can write the cluster operator as a sum of the two operators \hat{T}_2 and \hat{T}_4 which generate one and two pairs of atoms respectively. We can write them as

$$\hat{T}_2 = t_2(t) \left(\hat{a}_{e,0} \hat{a}_{g,p}^\dagger \right)^2 = t_2(t) \hat{S}^2 \quad (83a)$$

$$\hat{T}_4 = t_4(t) \left(\hat{a}_{e,0} \hat{a}_{g,p}^\dagger \right)^4 = t_4(t) \hat{S}^4 \quad (83b)$$

where we have used the operator $\hat{S} \equiv \hat{a}_{e,0} \hat{a}_{g,p}^\dagger$. In this manner we can write the cluster operator in the compact form

$$\hat{T} = t_2(t) \hat{S}^2 + t_4(t) \hat{S}^4. \quad (84)$$

To make up the coupled-cluster equations, which we will use to calculate the cluster amplitudes t_2 and t_4 , it is useful to write the Hamiltonian of this two-mode model also in terms of the operator \hat{S} that yields

$$\hat{H} = \kappa \left(\hat{a}_{g,p}^\dagger \hat{a}_{g,p}^\dagger \hat{a}_{e,0} \hat{a}_{e,0} + \hat{a}_{e,0} \hat{a}_{e,0} \hat{a}_{g,p}^\dagger \hat{a}_{g,p}^\dagger \right) = \kappa \left[\left(\hat{S}^\dagger \right)^2 + \hat{S}^2 \right] \quad (85)$$

which is in analogy to what we already had in (60). Due to the truncation of the cluster operator \hat{T} (see (82)) we get two independent, coupled equations for the variables t_2 and t_4 which are

$$i \langle \phi_0 | \left(\hat{S}^\dagger \right)^2 e^{-\hat{T}} \frac{\partial}{\partial t} e^{\hat{T}} | \phi_0 \rangle = \langle \phi_0 | \left(\hat{S}^\dagger \right)^2 e^{-\hat{T}} H e^{\hat{T}} | \phi_0 \rangle \quad (86a)$$

$$i \langle \phi_0 | \left(\hat{S}^\dagger \right)^4 e^{-\hat{T}} \frac{\partial}{\partial t} e^{\hat{T}} | \phi_0 \rangle = \langle \phi_0 | \left(\hat{S}^\dagger \right)^4 e^{-\hat{T}} H e^{\hat{T}} | \phi_0 \rangle. \quad (86b)$$

To evaluate these equations we will make use of the expansion

$$\hat{A} \equiv e^{-\hat{T}} \hat{A} e^{\hat{T}} = \hat{A} + \frac{1}{1!} [\hat{A}, \hat{T}] + \frac{1}{2!} [[\hat{A}, \hat{T}], \hat{T}] + \dots \quad (87)$$

what for the term on the right hand side gives

$$e^{-\hat{T}} \frac{\partial}{\partial t} e^{\hat{T}} = e^{-\hat{T}} \dot{\hat{T}} e^{\hat{T}} = \dot{\hat{T}} = \dot{t}_2(t) \hat{S}^2 + \dot{t}_4(t) \hat{S}^4 \quad (88)$$

since the commutator $[\dot{\hat{T}}, \hat{T}]$ vanishes. And the coupled-cluster equations simplify to

$$i \langle \phi_0 | (\hat{S}^\dagger)^2 \frac{\partial}{\partial t} \hat{T} | \phi_0 \rangle = \langle \phi_0 | (\hat{S}^\dagger)^2 e^{-\hat{T}} H e^{\hat{T}} | \phi_0 \rangle \quad (89a)$$

$$i \langle \phi_0 | (\hat{S}^\dagger)^4 \frac{\partial}{\partial t} \hat{T} | \phi_0 \rangle = \langle \phi_0 | (\hat{S}^\dagger)^4 e^{-\hat{T}} H e^{\hat{T}} | \phi_0 \rangle. \quad (89b)$$

Also for the terms on the left hand side, equation (87) gives an exact expression and the coupled-cluster equations finally yield

$$\begin{aligned} i \dot{t}_2 \langle \phi_0 | (\hat{S}^\dagger)^2 \hat{S}^2 | \phi_0 \rangle &= \\ &= \kappa \langle \phi_0 | (\hat{S}^\dagger)^2 \hat{S}^2 | \phi_0 \rangle + \kappa t_4 \langle \phi_0 | (\hat{S}^\dagger)^4 \hat{S}^4 | \phi_0 \rangle + \\ &+ \frac{1}{2} \kappa t_2^2 \langle \phi_0 | (\hat{S}^\dagger)^4 \hat{S}^4 | \phi_0 \rangle - \kappa t_2^2 \langle \phi_0 | (\hat{S}^\dagger)^2 \hat{S}^2 (\hat{S}^\dagger)^2 \hat{S}^2 | \phi_0 \rangle \end{aligned} \quad (90a)$$

$$\begin{aligned} i \dot{t}_4 \langle \phi_0 | (\hat{S}^\dagger)^4 \hat{S}^4 | \phi_0 \rangle &= \\ &= \kappa t_2 t_4 \langle \phi_0 | (\hat{S}^\dagger)^6 \hat{S}^6 | \phi_0 \rangle - \kappa t_2 t_4 \langle \phi_0 | (\hat{S}^\dagger)^4 \hat{S}^2 (\hat{S}^\dagger)^2 \hat{S}^4 | \phi_0 \rangle + \\ &- \frac{1}{2} \kappa t_2^3 \langle \phi_0 | (\hat{S}^\dagger)^4 \hat{S}^2 (\hat{S}^\dagger)^2 \hat{S}^4 | \phi_0 \rangle - \kappa t_2 t_4 \langle \phi_0 | (\hat{S}^\dagger)^4 \hat{S}^4 (\hat{S}^\dagger)^2 \hat{S}^2 | \phi_0 \rangle + \\ &+ \frac{1}{2} \kappa t_2^3 \langle \phi_0 | (\hat{S}^\dagger)^4 \hat{S}^4 (\hat{S}^\dagger)^2 \hat{S}^2 | \phi_0 \rangle + \frac{1}{6} \kappa t_2^3 \langle \phi_0 | (\hat{S}^\dagger)^6 \hat{S}^6 | \phi_0 \rangle. \end{aligned} \quad (90b)$$

Now this system of coupled differential equations can be easily solved numerically, since the expectation values of excitation operators of the form $\langle \phi_0 | (\hat{S}^\dagger)^2 \hat{S}^2 | \phi_0 \rangle$ can be calculated (they are listed in appendix B.1).

If the cluster-amplitudes are calculated the wave function can be evaluated at the different time-steps of the simulation with equation (80). The expectation value of the pseudo-spin operator \hat{L}_z then gives the population density of the state (g, p) as already implemented in section 6.3.4. The result for a simulation of a system of $N = 100$ atoms is shown in figure 18 where it is compared to further truncations of the cluster operator, namely $\hat{T} = \hat{T}_2$ and $\hat{T} = \hat{T}_2 + \hat{T}_4 + \hat{T}_6$ and the exact solution obtained from the Schrödinger equation. The comparison shows that with the coupled-cluster theory we just obtain a perturbation series and that this approach is not a better alternative to the density matrix formalism applied in section 6.3.3.

6.6 Multi-mode model

Since we have tested different approaches for a two-mode model of the twin-atom beam generation, we found out that a first-order approximation within the density-matrix approach provides the best results and therefore, we will generalize this formalism to a multi-mode model in the following section.

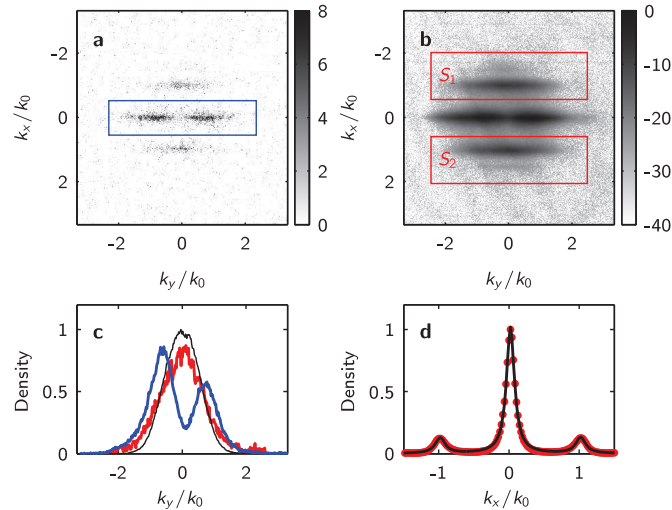


Figure 19: Results from the twin-atom beam experiment [1] which show momentum distributions of about 700 atoms released from the trap 7 ms (in (a),(b) and (d)) and 6 ms (in (c)) after starting the excitation sequence. (a) Momentum distribution gained by fluorescence detection (in photons per pixel). (b) Average of approximately 1500 images similar to (a). (c) Normalized, radial momentum distributions of the central (blue) and emitted (red) clouds (averaged over 50 images) in comparison to the distribution of a non-excited cloud (black). (d) Normalized profile of (b) along the x-direction (red dots) and three-peak Lorentzian fit (black line).

Figure (19) shows that a two-mode with just a single longitudinal mode $|g, \pm p\rangle$ being populated by the emitted atoms is not sufficient to describe the experiment adequately, but a variety of modes with energies centered around $E_{e,0}$ has to be depicted. While an extension of the full Schrödinger equation (in section 6.3.2) to a multi-mode model is impracticable, due to the exponentially increasing size of the Hilbert space, the generalization of the density matrix approach (in section 6.3.3) is straightforward and the multi-mode Hamiltonian for the non-linear coupling, describing the emission-process, takes the form

$$\hat{H}' = \frac{1}{2} \sum_{ij} \kappa_{ij} \left(\hat{a}_{g,i}^\dagger \hat{a}_{g,j}^\dagger \hat{a}_{e,0} \hat{a}_{e,0} + \hat{a}_{e,0}^\dagger \hat{a}_{e,0}^\dagger \hat{a}_{g,i} \hat{a}_{g,j} \right) \quad (91)$$

where the coupling matrix element between the source and the longitudinal

modes κ_{ij} can be expressed as

$$\kappa_{ij} = g \int \phi_i^*(x) \phi_j^*(x) \phi_g(x)^2 dx \int \phi_g^*(y)^2 \phi_e(y)^2 dy \int |\phi_g(z)|^4 dz \quad (92)$$

which is simply the generalization of equation (42). The wave functions $\phi_i(x) \phi_g(y) \phi_g(z)$ are those corresponding to the several longitudinal excited modes which are populated during emission. Since $\kappa_{ij} = \kappa_{ji}$ momentum conservation is fulfilled, and due to the symmetry of the single-particle wave functions also parity is conserved. Considering only this non-linear part of the Hamiltonian the equations of motion for the one-particle density matrices $\rho_{e,0} = \langle \hat{a}_{e,0}^\dagger \hat{a}_{e,0} \rangle$ and $\rho_{g,ij} = \langle \hat{a}_{g,i}^\dagger \hat{a}_{g,j} \rangle$ yield

$$i \left(\dot{\rho}_{ee}^{00} \right)' = \left\langle \left[\hat{a}_{e,0}^\dagger \hat{a}_{e,0}, \hat{H}' \right] \right\rangle = -2i \sum_{ij} \kappa_{ij} \text{Im} \Delta_{gg,ee}^{ij} \quad (93a)$$

$$i \left(\dot{\rho}_{gg}^{ij} \right)' = \left\langle \left[\hat{a}_{g,i}^\dagger \hat{a}_{g,j}, \hat{H}' \right] \right\rangle = \sum_k \left(\kappa_{jk} \Delta_{gg,ee}^{ik} - \kappa_{ik} \Delta_{gg,ee}^{*jk} \right), \quad (93b)$$

where $\Delta_{gg,ee}^{ij} = \langle \hat{a}_{g,i}^\dagger \hat{a}_{g,j}^\dagger \hat{a}_{e,0} \hat{a}_{e,0} \rangle$ is the two-particle coherence, whose time evolution is

$$i \left(\dot{\Delta}_{gg,ee}^{ij} \right)' \simeq \left(2\rho_{ee}^{00} + 1 \right) \sum_{kl} \kappa_{kl} \rho_{gg}^{ik} \rho_{gg}^{jl} - \kappa_{ij} \rho_{ee}^{00} \left(\rho_{ee}^{00} - 1 \right) + \\ - \rho_{ee}^{00} \left(\rho_{ee}^{00} - 1 \right) \sum_k \left(\kappa_{ik} \rho_{gg}^{jk} + \kappa_{jk} \rho_{gg}^{ik} \right). \quad (94)$$

To gain a complete description of the twin-atom beam generation process we also have to formulate the free time-evolution and the pumping process in terms of our multi-mode model which is covered by the Hamiltonian

$$\hat{H}_0 = \sum_{\mu=g,e} E_{\mu,0} \hat{a}_{\mu,0}^\dagger \hat{a}_{\mu,0} + \sum_i E_{g,i} \hat{a}_{g,i}^\dagger \hat{a}_{g,i} + \\ - \wp_{eg} \dot{y}_0 \left(\hat{a}_{e,0}^\dagger \hat{a}_{g,0} + \hat{a}_{g,0}^\dagger \hat{a}_{e,0} \right) - \wp_{eg} \dot{y}_0 \sum_i \left(\hat{a}_{e,i}^\dagger \hat{a}_{g,i} + \hat{a}_{g,i}^\dagger \hat{a}_{e,i} \right) \quad (95)$$

where the index i runs over the longitudinal excited modes with $E_{g,i} \simeq E_{e,0}$ and \wp is the momentum matrix element between the longitudinal ground and excited state.

Taking also into account the free evolution and the pumping, we additionally have to calculate the system of equations for the time evolution due to \hat{H}_0 , which for the single-particle density matrices yields

$$i \left(\dot{\rho}_{ee}^{00} \right)^0 = -i \wp \dot{y}_0 2 \text{Im} \rho_{eg}^{00} \quad (96a)$$

$$i \left(\dot{\rho}_{ge}^{ij} \right)^0 = \left(-E_{g,i} - E_{e,j} \right) \rho_{ge}^{ij} - \wp_{eg} \dot{y}_0 \left(\rho_{gg}^{ij} - \rho_{ee}^{ij} \right) \quad (96b)$$

and

$$i \left(\dot{\Delta}_{gg,ee}^{ij} \right)^0 = \left\langle \left[\hat{a}_{g,i}^\dagger \hat{a}_{g,j}^\dagger \hat{a}_{e,0} \hat{a}_{e,0}, \hat{H}_0 \right] \right\rangle = \\ = \Delta_{gg,ee}^{ij} (2E_{e,0} - E_{g,i} - E_{g,j}) - \wp_{eg} \dot{y}_0 \left(2\Delta_{gg,eg}^{ij} - \Delta_{eg,ee}^{ij} - \Delta_{ge,ee}^{ij} \right). \quad (97)$$

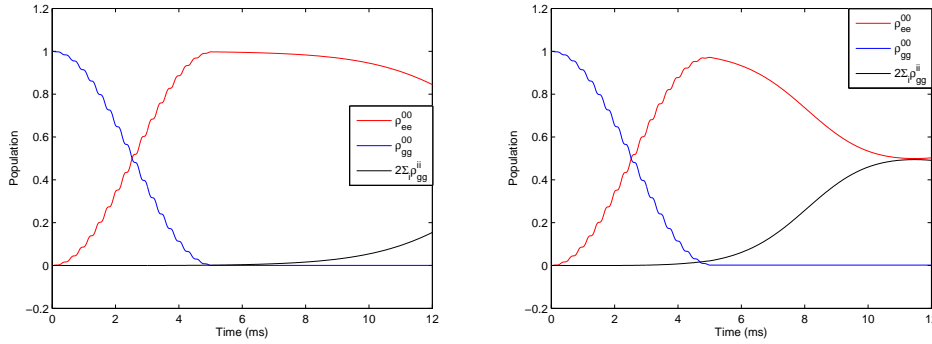


Figure 20: Simulation for one (left) and five (right) wing modes where the values for the coupling constants κ_{ij} and energies are calculated from the effective potential used in the experiment and a dephasing of $T_2 = 2\text{ms}$ for the two-particle density matrices is considered.

for the two-particle density matrix, just to name a few. The complete set of equations of motion for the one- and two-particle density matrices is listed in appendix A.2.

In figure 20 a simulation for one and five wing modes (g, i) respectively is shown, where the corresponding energies $E_{g,i}$ and the coupling matrix elements κ_{ij} are calculated from the effective Hamiltonian obtained in section (6.2). Additionally a dephasing of $T_2 = 2\text{ms}$ of the two-particle density matrix is taken into account. For the displacement of the potential minimum, responsible for the transfer of the condensate from the transversal ground $(g, 0)$ to the first excited state $(e, 0)$, a trajectory of $y_0(t) = -0.022 \sin(E_{e,0}t)$ active at the first 5ms of the simulation, was used and a value of $\wp_{eg} = -2.45$ for the momentum matrix element was used. The simulation was run for $N = 700$ particles.

6.7 Conclusion and outlook

Within this thesis a model for the generation of twin-atom beams, emitted from a one-dimensional degenerate Bose gas in the first radial excited state of an elongated trap, was developed. In a first approach, a two-mode model is used to describe the population of a single twin-mode by atom-pairs emitted from the quasi-BEC. This problem allows a full numerical solution of the corresponding Schrödinger equation, which is compared to the results obtained from a density matrix and a coupled-cluster approach. For the density matrix approach different factorization schemes to truncate the BBGKY hierarchy of equations of motion are probed. The density matrix approach is then applied to a multi-mode model, where several twin-modes are populated. Also the pumping process, where the quasi-condensate is transferred from the ground to the first excited state of the waveguide potential, is modeled in this approach.

Furthermore, the effect of the thermal occupation of the twin-modes as

seeds for the emission, as well as an adequate treatment of the non-condensed particles in the GPE, including the corresponding changes of the interaction matrix elements, and the energies of the modes could be investigated.

References

- [1] R. Bücker, J. Grond, S. Manz, T. Berrada, T. Betz, C. Koller, U. Hohenester, T. Schumm, A. Perrin, and J. Schmiedmayer, *Nature Physics* **7**, 8 (2010), URL <http://arxiv.org/abs/1012.2348>.
- [2] A. Einstein, *Sitzungsber. Preuss. Akad. Wiss. Bericht* **22**, 261 (1924).
- [3] A. Einstein, *Sitzungsber. Preuss. Akad. Wiss. Bericht* **1**, 3 (1925).
- [4] O. Penrose and L. Onsager, *Phys. Rev.* **104**, 576 (1956), URL <http://link.aps.org/doi/10.1103/PhysRev.104.576>.
- [5] P. W. Courteille, V. S. Bagnato, and V. I. Yukalov, *Laser Physics* **11**, 200 (2001), URL <http://arxiv.org/abs/cond-mat/0109421>.
- [6] E. P. Gross, *Il Nuovo Cimento* **20**, 454 (1961).
- [7] L. P. Pitaevskii, *Sov. Phys.-JETP* **13**, 451 (1961).
- [8] D. S. Petrov, G. V. Shlyapnikov, and J. T. M. Walraven, *Phys. Rev. Lett.* **85**, 3745 (2000), URL <http://link.aps.org/doi/10.1103/PhysRevLett.85.3745>.
- [9] A. Görlitz, J. M. Vogels, A. E. Leanhardt, C. Raman, T. L. Gustavson, J. R. Abo-Shaeer, A. P. Chikkatur, S. Gupta, S. Inouye, T. Rosenband, et al., *Phys. Rev. Lett.* **87**, 130402 (2001), URL <http://link.aps.org/doi/10.1103/PhysRevLett.87.130402>.
- [10] P. C. Hohenberg, *Phys. Rev.* **158**, 383 (1967), URL <http://link.aps.org/doi/10.1103/PhysRev.158.383>.
- [11] N. D. Mermin and H. Wagner, *Phys. Rev. Lett.* **17**, 1133 (1966), URL <http://link.aps.org/doi/10.1103/PhysRevLett.17.1133>.
- [12] L. Pitaevskii and S. Stringari, *Journal of Low Temperature Physics* **85**, 377 (1991), ISSN 0022-2291, 10.1007/BF00682193, URL <http://dx.doi.org/10.1007/BF00682193>.
- [13] V. Bagnato and D. Kleppner, *Phys. Rev. A* **44**, 7439 (1991), URL <http://link.aps.org/doi/10.1103/PhysRevA.44.7439>.
- [14] W. Ketterle and N. J. van Druten, *Phys. Rev. A* **54**, 656 (1996), URL <http://link.aps.org/doi/10.1103/PhysRevA.54.656>.
- [15] E. L. Raab, M. Prentiss, A. Cable, S. Chu, and D. E. Pritchard, *Phys. Rev. Lett.* **59**, 2631 (1987), URL <http://link.aps.org/doi/10.1103/PhysRevLett.59.2631>.
- [16] W. D. Phillips, *Nobelprize.org* (1997), URL http://www.nobelprize.org/nobel_prizes/physics/laureates/1997/phillips-lecture.html.

-
- [17] W. Ketterle, D. S. Durfee, and D. M. Stamper-Kurn, *Making, probing and understanding bose-einstein condensates* (1999), URL <http://www.citebase.org/abstract?id=oai:arXiv.org:cond-mat/9904034>.
- [18] R. Bücker, A. Perrin, S. Manz, T. Betz, C. Koller, T. Plisson, J. Rottmann, T. Schumm, and J. Schmiedmayer, *NEW J.PHYS.* **11**, 103039 (2009), URL <http://arxiv.org/pdf/0907.0674v2.pdf>.
- [19] R. Folman, P. Krüger, J. Schmiedmayer, J. Denschlag, and C. Henkel (Academic Press, 2002), vol. 48 of *Advances In Atomic, Molecular, and Optical Physics*, pp. 263 – 356, URL <http://arxiv.org/pdf/0805.2613v1.pdf>.
- [20] W. Hänsel, P. Hommelhoff, T. W. Hänsch, and J. Reichel, *Nature* **413**, 498 (2001).
- [21] H. Ott, J. Fortagh, G. Schlotterbeck, A. Grossmann, and C. Zimmermann, *Phys. Rev. Lett.* **87**, 230401 (2001), URL <http://link.aps.org/doi/10.1103/PhysRevLett.87.230401>.
- [22] W. Ketterle and D. E. Pritchard, *Applied Physics B: Lasers and Optics* **54**, 403 (1992), ISSN 0946-2171, 10.1007/BF00325386, URL <http://dx.doi.org/10.1007/BF00325386>.
- [23] J. Fortágh and C. Zimmermann, *Rev. Mod. Phys.* **79**, 235 (2007), URL <http://link.aps.org/doi/10.1103/RevModPhys.79.235>.
- [24] J. D. Weinstein and K. G. Libbrecht, *Phys. Rev. A* **52**, 4004 (1995), URL <http://link.aps.org/doi/10.1103/PhysRevA.52.4004>.
- [25] T. Schumm, S. Hofferberth, L. M. Andersson, S. Wildermuth, S. Groth, I. Bar-Joseph, J. Schmiedmayer, and P. Krüger, *Nature Physics* **1**, 57 (2005), URL <http://www.nature.com/doi/10.1038/nphys125>.
- [26] R. Bücker, *Quanten-Zwillinge aus dem Atomchip*, <http://tuweb.tuwien.ac.at/index.php?id=11257> (2011), copyright TU Wien.
- [27] A. Heidmann, R. J. Horowicz, S. Reynaud, E. Giacobino, C. Fabre, and G. Camy, *Phys. Rev. Lett.* **59**, 2555 (1987), URL <http://link.aps.org/doi/10.1103/PhysRevLett.59.2555>.
- [28] U. Hohenester, P. K. Rekdal, A. Borzi, and J. Schmiedmayer, *Phys. Rev. A* **75**, 023602 (2007), URL <http://link.aps.org/doi/10.1103/PhysRevA.75.023602>.
- [29] K. Sakmann, *Many-Body Schrödinger Dynamics of Bose-Einstein Condensates*, Springer Theses (Springer, 2011), ISBN 9783642228650.
- [30] J. R. Anglin and A. Vardi, *Phys. Rev. A* **64**, 013605 (2001), URL <http://link.aps.org/doi/10.1103/PhysRevA.64.013605>.
- [31] A. Vardi and J. R. Anglin, *Phys. Rev. Lett.* **86**, 568 (2001), URL <http://link.aps.org/doi/10.1103/PhysRevLett.86.568>.

-
- [32] F. T. Arecchi, E. Courtens, R. Gilmore, and H. Thomas, Phys. Rev. A **6**, 2211 (1972), URL <http://link.aps.org/doi/10.1103/PhysRevA.6.2211>.
- [33] F. Coester, Nuclear Physics **7**, 421 (1958), ISSN 0029-5582, URL <http://www.sciencedirect.com/science/article/pii/0029558258902803>.
- [34] F. Coester and H. Kümmel, Nuclear Physics **17**, 477 (1960), ISSN 0029-5582, URL <http://www.sciencedirect.com/science/article/pii/0029558260901401>.
- [35] L. S. Cederbaum, O. E. Alon, and A. I. Streltsov, Phys. Rev. A **73**, 043609 (2006), URL <http://link.aps.org/doi/10.1103/PhysRevA.73.043609>.

Appendices

A Heisenberg equations of motion

We calculate the time evolution of the one- and two-particle density matrices ρ and Δ through the Heisenberg equations of motion $i\dot{\rho} = \langle [\rho, \hat{H}] \rangle$ and $i\dot{\Delta} = \langle [\Delta, \hat{H}] \rangle$ respectively. The Hamiltonian $\hat{H} = \hat{H}_0 + \hat{H}'$ with \hat{H}_0 , containing the free time evolution and the pumping process, and \hat{H}' , describing the atom-atom interaction responsible for the emission of the twin-atom beams. Through \hat{H}' the time evolution of the one-particle density matrices depends on the two-particle density matrices and that of the two-particle density matrices on the three-particle density matrices and so on. To obtain a closed set of equations, we approximate the three-particle density matrices by products of one-particle density matrices (see A.1.1) and, alternatively, by a sum of products of one- and two-particle density matrices (see A.1.2).

A.1 Two-mode model

The process of the emission of twin-atom beams is mapped onto a two-mode model, where only a single longitudinal excited mode $(g, \pm p)$ with $E_{e,0} = E_{g,p}$ can be populated. This model contains the transversal excited state $(e, 0)$ and the twin-atom states $(g, \pm p)$. Additionally, the states $(g, 0)$ and $(e, \pm p)$ are included, since also the pumping process is taken into account.

A.1.1 First-order approximation

In this approach the three-particle density matrices are factorized according to $\langle ABC \rangle \simeq \langle A \rangle \langle B \rangle \langle C \rangle$, where A , B and C are pairs of creation and annihilation operators.

One-particle density matrices

$$i\dot{\rho}_{gg,0} = \left\langle \left[\hat{a}_{g,0}^\dagger \hat{a}_{g,0}, \hat{H}_0 + \hat{H}' \right] \right\rangle = i\wp_{eg}\dot{y}_0 2 \text{Im } \rho_{eg,0} \quad (98a)$$

$$i\dot{\rho}_{ee,0} = -i\wp_{eg}\dot{y}_0 2 \text{Im } \rho_{eg,0} - 4i\kappa \text{Im } \Delta_{gg,ee} \quad (98b)$$

$$i\dot{\rho}_{eg,0} = (E_{g,0} - E_{e,0})\rho_{eg,0} - \wp_{eg}\dot{y}_0(\rho_{ee,0} - \rho_{gg,0}) - 2\kappa\Delta_{gg,eg} \quad (98c)$$

$$i\dot{\rho}_{gg,p} = i\wp_{eg}\dot{y}_0 2 \operatorname{Im} \rho_{eg,p} + 2i\kappa \operatorname{Im} \Delta_{gg,ee} \quad (98d)$$

$$i\dot{\rho}_{ee,p} = -i\wp_{eg}\dot{y}_0 2 \operatorname{Im} \rho_{eg,p} \quad (98e)$$

$$i\dot{\rho}_{eg,p} = (E_{g,p} - E_{e,p})\rho_{eg,p} - \wp_{eg}\dot{y}_0(\rho_{ee,p} - \rho_{gg,p}) + \kappa\Delta_{eg,ee}. \quad (98f)$$

Two-particle density matrices

$$\begin{aligned} i\dot{\Delta}_{gg,ee} &\simeq \left\langle \left[\hat{a}_{g,p}^\dagger \hat{a}_{g,-p}^\dagger \hat{a}_{e,0} \hat{a}_{e,0} \hat{H}_0 \right] \right\rangle = \\ &= 2\Delta_{gg,ee} (E_{e,0} - E_{g,p}) - 2\wp_{eg}\dot{y}_0 (\Delta_{gg,eg} - \Delta_{eg,ee}) + \\ &\quad + 2\kappa\rho_{gg,p}^2 (2\rho_{ee,0} + 1) - \kappa (2\rho_{gg,p} + 1) \rho_{ee,0} (\rho_{ee,0} - 1) \end{aligned} \quad (99a)$$

$$\begin{aligned} i\dot{\Delta}_{gg,eg} &\simeq \Delta_{gg,eg} (E_{e,0} + E_{g,0} - 2E_{g,p}) - \wp_{eg}\dot{y}_0 (\Delta_{gg,gg} + \Delta_{gg,ee} - 2\Delta_{eg,eg}) + \\ &\quad + 2\kappa\rho_{gg,p}^2 \rho_{eg,0} - \kappa (2\rho_{gg,p} + 1) \rho_{ee,0} \rho_{eg,0} \end{aligned} \quad (99b)$$

$$\begin{aligned} i\dot{\Delta}_{gg,gg} &\simeq 2\Delta_{gg,gg} (E_{g,0} - E_{g,p}) - 2\wp_{eg}\dot{y}_0 (\Delta_{gg,eg} - \Delta_{eg,gg}) + \\ &\quad - \kappa (2\rho_{gg,p} + 1) \rho_{eg,0}^2 \end{aligned} \quad (99c)$$

$$\begin{aligned} i\dot{\Delta}_{eg,ee} &\simeq \Delta_{eg,ee} (2E_{e,0} - E_{g,p} - E_{e,p}) - \wp_{eg}\dot{y}_0 (2\Delta_{eg,eg} - \Delta_{gg,ee} - \Delta_{ee,ee}) + \\ &\quad + 2\kappa\rho_{eg,p}\rho_{gg,p} (2\rho_{ee,0} + 1) - \kappa\rho_{eg,p}\rho_{ee,0} (\rho_{ee,0} - 1) \end{aligned} \quad (99d)$$

$$\begin{aligned} i\dot{\Delta}_{eg,eg} &\simeq \Delta_{eg,eg} (E_{e,0} + E_{g,0} - E_{g,p} - E_{e,p}) + \\ &\quad - \wp_{eg}\dot{y}_0 (\Delta_{eg,gg} + \Delta_{eg,ee} - \Delta_{gg,eg} - \Delta_{ee,eg}) + \\ &\quad + 2\kappa\rho_{eg,p}\rho_{gg,p}\rho_{eg,0} - \kappa\rho_{eg,p}\rho_{ee,0}\rho_{eg,0} \end{aligned} \quad (99e)$$

$$\begin{aligned} i\dot{\Delta}_{eg,gg} &\simeq \Delta_{eg,gg} (2E_{g,0} - E_{g,p} - E_{e,p}) - \wp_{eg}\dot{y}_0 (2\Delta_{eg,eg} - \Delta_{gg,gg} - \Delta_{ee,gg}) + \\ &\quad - \kappa\rho_{eg,p}\rho_{eg,0}^2 \end{aligned} \quad (99f)$$

$$\begin{aligned} i\dot{\Delta}_{ee,ee} &\simeq 2\Delta_{ee,ee} (E_{e,0} - E_{e,p}) - 2\wp_{eg}\dot{y}_0 (\Delta_{ee,eg} - \Delta_{eg,ee}) + \\ &\quad + 2\kappa\rho_{eg,p}^2 (2\rho_{ee,0} + 1) \end{aligned} \quad (99g)$$

$$\begin{aligned} i\dot{\Delta}_{ee,eg} &\simeq \Delta_{ee,eg} (E_{e,0} + E_{g,0} - 2E_{e,p}) - \wp_{eg}\dot{y}_0 (\Delta_{ee,gg} + \Delta_{ee,ee} - 2\Delta_{eg,eg}) + \\ &\quad + 2\kappa\rho_{eg,p}^2 \rho_{eg,0} \end{aligned} \quad (99h)$$

$$i\dot{\Delta}_{ee,gg} = 2\Delta_{ee,gg} (E_{g,0} - E_{e,p}) - 2\wp_{eg}\dot{y}_0 (\Delta_{ee,eg} - \Delta_{eg,gg}) \quad (99i)$$

A.1.2 Second-order approximation

Here we also include the coupling terms between one- and two-particle density matrices in the factorization and approximate the three-particle density matrices by

$$\langle ABC \rangle \simeq \langle AB \rangle \langle C \rangle + \langle A \rangle \langle BC \rangle + \langle AC \rangle \langle B \rangle - 2 \langle A \rangle \langle B \rangle \langle C \rangle. \quad (100)$$

Within this approach we just consider the emission process and hence solely the time evolution of the density matrices due to \hat{H}' . While for the one-particle density matrix $\rho_{ee,0}$ the equation of motion stays unchanged, that of the two-particle density matrix $\Delta_{gg,ee}$ becomes

$$\begin{aligned} \langle [\hat{a}_{g,p}^\dagger \hat{a}_{g,-p}^\dagger \hat{a}_{e,0} \hat{a}_{e,0}, \hat{H}'] \rangle &\simeq 4\kappa \langle \hat{a}_{g,p}^\dagger \hat{a}_{g,-p}^\dagger \hat{a}_{g,p} \hat{a}_{g,-p} \rangle \langle \hat{a}_{e,0}^\dagger \hat{a}_{e,0} \rangle + \\ &+ 8\kappa \langle \hat{a}_{g,p}^\dagger \hat{a}_{g,p} \rangle \langle \hat{a}_{g,p}^\dagger \hat{a}_{e,0}^\dagger \hat{a}_{g,p} \hat{a}_{e,0} \rangle - 8\kappa \langle \hat{a}_{g,p}^\dagger \hat{a}_{g,p} \rangle^2 \langle \hat{a}_{e,0}^\dagger \hat{a}_{e,0} \rangle + \\ &+ 2\kappa \langle \hat{a}_{g,p}^\dagger \hat{a}_{g,-p}^\dagger \hat{a}_{g,p} \hat{a}_{g,-p} \rangle - 4\kappa \langle \hat{a}_{e,0}^\dagger \hat{a}_{g,p}^\dagger \hat{a}_{e,0} \hat{a}_{g,p} \rangle \langle \hat{a}_{e,0}^\dagger \hat{a}_{e,0} \rangle + \\ &- 2\kappa \langle \hat{a}_{g,p}^\dagger \hat{a}_{g,p} \rangle \langle \hat{a}_{e,0}^\dagger \hat{a}_{e,0}^\dagger \hat{a}_{e,0} \hat{a}_{e,0} \rangle + 4\kappa \langle \hat{a}_{g,p}^\dagger \hat{a}_{g,p} \rangle \langle \hat{a}_{e,0}^\dagger \hat{a}_{e,0} \rangle^2 + \\ &- \kappa \langle \hat{a}_{e,0}^\dagger \hat{a}_{e,0}^\dagger \hat{a}_{e,0} \hat{a}_{e,0} \rangle \end{aligned} \quad (101)$$

and now depends on further two-particle density matrices for which the time evolution is given by

$$\begin{aligned} \langle [\hat{a}_{g,p}^\dagger \hat{a}_{g,-p}^\dagger \hat{a}_{g,p} \hat{a}_{g,-p}, \hat{H}'] \rangle &\simeq 2\kappa \langle \hat{a}_{g,p}^\dagger \hat{a}_{g,p} \rangle \langle \hat{a}_{g,p}^\dagger \hat{a}_{g,-p}^\dagger \hat{a}_{e,0} \hat{a}_{e,0} \rangle + \\ &+ \kappa \langle \hat{a}_{g,p}^\dagger \hat{a}_{g,-p}^\dagger \hat{a}_{e,0} \hat{a}_{e,0} \rangle - 2\kappa \langle \hat{a}_{g,p}^\dagger \hat{a}_{g,p} \rangle \langle \hat{a}_{e,0}^\dagger \hat{a}_{e,0}^\dagger \hat{a}_{g,p} \hat{a}_{g,-p} \rangle + \\ &- \kappa \langle \hat{a}_{e,0}^\dagger \hat{a}_{e,0}^\dagger \hat{a}_{g,p} \hat{a}_{g,-p} \rangle \end{aligned} \quad (102a)$$

$$\begin{aligned} \langle [\hat{a}_{g,p}^\dagger \hat{a}_{e,0}^\dagger \hat{a}_{g,p} \hat{a}_{e,0}, \hat{H}'] \rangle &\simeq \kappa \langle \hat{a}_{e,0}^\dagger \hat{a}_{e,0} \rangle \langle \hat{a}_{g,p}^\dagger \hat{a}_{g,-p}^\dagger \hat{a}_{e,0} \hat{a}_{e,0} \rangle + \\ &+ 2\kappa \langle \hat{a}_{g,p}^\dagger \hat{a}_{g,p} \rangle \langle \hat{a}_{e,0}^\dagger \hat{a}_{e,0}^\dagger \hat{a}_{g,p} \hat{a}_{g,-p} \rangle - \kappa \langle \hat{a}_{e,0}^\dagger \hat{a}_{e,0} \rangle \langle \hat{a}_{e,0}^\dagger \hat{a}_{e,0}^\dagger \hat{a}_{g,p} \hat{a}_{g,-p} \rangle \end{aligned} \quad (102b)$$

$$\begin{aligned} \langle [\hat{a}_{e,0}^\dagger \hat{a}_{e,0}^\dagger \hat{a}_{e,0} \hat{a}_{e,0}, \hat{H}'] \rangle &\simeq -4\kappa \langle \hat{a}_{e,0}^\dagger \hat{a}_{e,0} \rangle \langle \hat{a}_{g,p}^\dagger \hat{a}_{g,-p}^\dagger \hat{a}_{e,0} \hat{a}_{e,0} \rangle + \\ &- 2\kappa \langle \hat{a}_{g,p}^\dagger \hat{a}_{g,-p}^\dagger \hat{a}_{e,0} \hat{a}_{e,0} \rangle + 4\kappa \langle \hat{a}_{e,0}^\dagger \hat{a}_{e,0} \rangle \langle \hat{a}_{e,0}^\dagger \hat{a}_{e,0}^\dagger \hat{a}_{g,p} \hat{a}_{g,-p} \rangle + \\ &+ 2\kappa \langle \hat{a}_{e,0}^\dagger \hat{a}_{e,0}^\dagger \hat{a}_{g,p} \hat{a}_{g,-p} \rangle. \end{aligned} \quad (102c)$$

A.1.3 Pseudospin-operator approach

Within this approach we solely model the emission process and consider the expectation values of the pseudospin-operators

$$\hat{L}_x \equiv \frac{\hat{a}_{e,0}^\dagger \hat{a}_{g,p} + \hat{a}_{g,p}^\dagger \hat{a}_{e,0}}{2} \quad (103a)$$

$$\hat{L}_y \equiv \frac{\hat{a}_{e,0}^\dagger \hat{a}_{g,p} - \hat{a}_{g,p}^\dagger \hat{a}_{e,0}}{2i} \quad (103b)$$

$$\hat{L}_z \equiv \frac{\hat{a}_{e,0}^\dagger \hat{a}_{e,0} - \hat{a}_{g,p}^\dagger \hat{a}_{g,p}}{2} \quad (103c)$$

instead of the one-particle density matrices. The equations of motion for this angular momentum operators are given by

$$\frac{d}{dt} \hat{L}_x = -i [\hat{L}_x, \hat{H}'] = -\kappa (\hat{L}_y \hat{L}_z + \hat{L}_z \hat{L}_y) \quad (104a)$$

$$\frac{d}{dt} \hat{L}_y = -i [\hat{L}_y, \hat{H}'] = -\kappa (\hat{L}_x \hat{L}_z + \hat{L}_z \hat{L}_x) \quad (104b)$$

$$\frac{d}{dt} \hat{L}_z = -i [\hat{L}_z, \hat{H}'] = 2\kappa (\hat{L}_x \hat{L}_y + \hat{L}_y \hat{L}_x) \quad (104c)$$

and also depend on the second order moments, for which the time evolution is given by

$$\begin{aligned} \frac{d}{dt} \langle \hat{L}_x \hat{L}_z \rangle &= -i \langle [\hat{L}_x \hat{L}_z, \hat{H}'] \rangle \simeq \\ &\simeq 6\kappa \langle \hat{L}_x \rangle \langle \hat{L}_x \hat{L}_y \rangle + 4\kappa \langle \hat{L}_y \rangle \langle \hat{L}_x \hat{L}_x \rangle + 2\kappa \langle \hat{L}_x \rangle \langle \hat{L}_y \hat{L}_x \rangle - 8\kappa \langle \hat{L}_x \rangle \langle \hat{L}_x \rangle \langle \hat{L}_y \rangle + \\ &\quad - 3\kappa \langle \hat{L}_z \rangle \langle \hat{L}_y \hat{L}_z \rangle - 2\kappa \langle \hat{L}_y \rangle \langle \hat{L}_z \hat{L}_z \rangle - \kappa \langle \hat{L}_z \hat{L}_y \rangle \langle \hat{L}_z \rangle + 4\kappa \langle \hat{L}_z \rangle \langle \hat{L}_z \rangle \langle \hat{L}_y \rangle \end{aligned} \quad (105a)$$

$$\begin{aligned} \frac{d}{dt} \langle \hat{L}_y \hat{L}_z \rangle &\simeq \\ &\simeq 6\kappa \langle \hat{L}_y \rangle \langle \hat{L}_y \hat{L}_x \rangle + 4\kappa \langle \hat{L}_x \rangle \langle \hat{L}_y \hat{L}_y \rangle + 2\kappa \langle \hat{L}_y \rangle \langle \hat{L}_x \hat{L}_y \rangle - 8\kappa \langle \hat{L}_x \rangle \langle \hat{L}_y \rangle \langle \hat{L}_y \rangle + \\ &\quad - 3\kappa \langle \hat{L}_z \rangle \langle \hat{L}_x \hat{L}_z \rangle - 2\kappa \langle \hat{L}_x \rangle \langle \hat{L}_z \hat{L}_z \rangle - \kappa \langle \hat{L}_z \hat{L}_x \rangle \langle \hat{L}_z \rangle + 4\kappa \langle \hat{L}_x \rangle \langle \hat{L}_z \rangle \langle \hat{L}_z \rangle \end{aligned} \quad (105b)$$

$$\begin{aligned} \frac{d}{dt} \langle \hat{L}_x \hat{L}_y \rangle &\simeq \\ &\simeq -3\kappa \langle \hat{L}_x \rangle \langle \hat{L}_x \hat{L}_z \rangle - 2\kappa \langle \hat{L}_z \rangle \langle \hat{L}_x \hat{L}_x \rangle - \kappa \langle \hat{L}_x \rangle \langle \hat{L}_z \hat{L}_x \rangle + 4\kappa \langle \hat{L}_x \rangle \langle \hat{L}_x \rangle \langle \hat{L}_z \rangle + \\ &\quad - 3\kappa \langle \hat{L}_y \rangle \langle \hat{L}_z \hat{L}_y \rangle - 2\kappa \langle \hat{L}_z \rangle \langle \hat{L}_y \hat{L}_y \rangle - \kappa \langle \hat{L}_y \hat{L}_z \rangle \langle \hat{L}_y \rangle + 4\kappa \langle \hat{L}_y \rangle \langle \hat{L}_y \rangle \langle \hat{L}_z \rangle \end{aligned} \quad (105c)$$

$$\begin{aligned} \frac{d}{dt} \langle \hat{L}_x \hat{L}_x \rangle &\simeq \\ &\simeq -2\kappa \langle \hat{L}_x \rangle \langle \hat{L}_z \hat{L}_y \rangle - 2\kappa \langle \hat{L}_x \rangle \langle \hat{L}_y \hat{L}_z \rangle - 2\kappa \langle \hat{L}_z \rangle \langle \hat{L}_x \hat{L}_y \rangle - 2\kappa \langle \hat{L}_z \rangle \langle \hat{L}_y \hat{L}_x \rangle + \end{aligned} \quad (105d)$$

$$- 2\kappa\langle\hat{L}_y\rangle\langle\hat{L}_x\hat{L}_z\rangle - 2\kappa\langle\hat{L}_y\rangle\langle\hat{L}_z\hat{L}_x\rangle + 8\kappa\langle\hat{L}_x\rangle\langle\hat{L}_y\rangle\langle\hat{L}_z\rangle$$

$$\frac{d}{dt}\langle\hat{L}_y\hat{L}_y\rangle \simeq \frac{d}{dt}\langle\hat{L}_x\hat{L}_x\rangle \quad (105e)$$

$$\begin{aligned} \frac{d}{dt}\langle\hat{L}_z\hat{L}_z\rangle &\simeq & (105f) \\ &\simeq 4\kappa\langle\hat{L}_x\rangle\langle\hat{L}_y\hat{L}_z\rangle + 4\kappa\langle\hat{L}_x\rangle\langle\hat{L}_z\hat{L}_y\rangle + 4\kappa\langle\hat{L}_y\rangle\langle\hat{L}_x\hat{L}_z\rangle + 4\kappa\langle\hat{L}_y\rangle\langle\hat{L}_z\hat{L}_x\rangle + \\ &\quad + 4\kappa\langle\hat{L}_z\rangle\langle\hat{L}_x\hat{L}_y\rangle + 4\kappa\langle\hat{L}_z\rangle\langle\hat{L}_y\hat{L}_x\rangle - 16\kappa\langle\hat{L}_x\rangle\langle\hat{L}_y\rangle\langle\hat{L}_z\rangle, \end{aligned}$$

if we apply the factorization $\langle\hat{L}_i\hat{L}_j\hat{L}_k\rangle \approx \langle\hat{L}_i\hat{L}_j\rangle\langle\hat{L}_k\rangle + \langle\hat{L}_i\rangle\langle\hat{L}_j\hat{L}_k\rangle + \langle\hat{L}_i\hat{L}_k\rangle\langle\hat{L}_j\rangle - 2\langle\hat{L}_i\rangle\langle\hat{L}_j\rangle\langle\hat{L}_k\rangle$ for the third order moments.

A.2 Multi-mode model

Here the two-mode model of the emission process is generalized to a multi-mode model in which the twin-atom beams can populate several modes (g, i) with energies centered around $E_{e,0}$.

A.2.1 Pumping and free time evolution

The Heisenberg equations of motion for the free time evolution and the time-dependent excitation (pumping) of the one-particle density matrices are given by

$$i \left(\dot{\rho}_{gg}^{00} \right)^0 = \left\langle \left[\hat{a}_{g,0}^\dagger \hat{a}_{g,0}, \hat{H}_0 \right] \right\rangle = i \wp_{eg} \dot{y}_0 2 \text{Im} \rho_{eg}^{00} \quad (106a)$$

$$i \left(\dot{\rho}_{ee}^{00} \right)^0 = -i \wp_{eg} \dot{y}_0 2 \text{Im} \rho_{eg}^{00} \quad (106b)$$

$$i \left(\dot{\rho}_{eg}^{00} \right)^0 = (E_{g,0} - E_{e,0}) \rho_{eg,0} - \wp_{eg} \dot{y}_0 \left(\rho_{ee}^{00} - \rho_{gg}^{00} \right) \quad (106c)$$

$$i \left(\dot{\rho}_{gg}^{ij} \right)^0 = (E_{g,i} - E_{g,j}) \rho_{gg}^{ij} + \wp_{eg} \dot{y}_0 \left(\rho_{eg}^{ij} - \left(\rho_{eg}^{ji} \right)^* \right) \quad (106d)$$

$$i \left(\dot{\rho}_{ee}^{ij} \right)^0 = (E_{e,j} - E_{e,i}) \rho_{ee}^{ij} - \wp_{eg} \dot{y}_0 \left(\rho_{eg}^{ij} - \left(\rho_{eg}^{ji} \right)^* \right) \quad (106e)$$

$$i \left(\dot{\rho}_{eg}^{ij} \right)^0 = (E_{g,j} - E_{e,i}) \rho_{eg}^{ij} - \wp_{eg} \dot{y}_0 \left(\rho_{ee}^{ij} - \rho_{gg}^{ij} \right). \quad (106f)$$

In the same manner the equations of motion for the two-particle density matrices can be calculated what gives

$$\begin{aligned} i \left(\dot{\Delta}_{gg,ee}^{ij} \right)^0 &= \left\langle \left[\hat{a}_{g,i}^\dagger \hat{a}_{g,j}^\dagger \hat{a}_{e,0} \hat{a}_{e,0}, \hat{H}_0 \right] \right\rangle = \\ &= \Delta_{gg,ee}^{ij} (2E_{e,0} - E_{g,i} - E_{g,j}) - \wp_{eg} \dot{y}_0 \left(2\Delta_{gg,eg}^{ij} - \Delta_{eg,ee}^{ij} - \Delta_{eg,ee}^{ji} \right) \end{aligned} \quad (107a)$$

$$\begin{aligned} i \left(\dot{\Delta}_{gg,eg}^{ij} \right)^0 &= \Delta_{gg,eg}^{ij} (E_{g,0} + E_{e,0} - E_{g,i} - E_{g,j}) + \\ &- \wp_{eg} \dot{y}_0 \left(\Delta_{gg,gg}^{ij} + \Delta_{gg,ee}^{ij} - \Delta_{eg,eg}^{ij} - \Delta_{eg,eg}^{ji} \right) \end{aligned} \quad (107b)$$

$$\begin{aligned} i \left(\dot{\Delta}_{gg,gg}^{ij} \right)^0 &= \Delta_{gg,gg}^{ij} (2E_{g,0} - E_{g,i} - E_{g,j}) + \\ &- \wp_{eg} \dot{y}_0 \left(2\Delta_{gg,eg}^{ij} - \Delta_{eg,gg}^{ij} - \Delta_{eg,gg}^{ji} \right) \end{aligned} \quad (107c)$$

$$i \left(\dot{\Delta}_{eg,ee}^{ij} \right)^0 = \Delta_{eg,ee}^{ij} (2E_{e,0} - E_{g,j} - E_{e,i}) + \quad (107d)$$

$$- \wp_{eg} \dot{y}_0 \left(2\Delta_{eg,eg}^{ij} - \Delta_{gg,ee}^{ij} - \Delta_{ee,ee}^{ij} \right)$$

$$i \left(\dot{\Delta}_{eg,eg}^{ij} \right)^0 = \Delta_{eg,eg}^{ij} (E_{g,0} + E_{e,0} - E_{g,j} - E_{e,i}) + \quad (107e)$$

$$- \wp_{eg} \dot{y}_0 \left(\Delta_{eg,gg}^{ij} + \Delta_{eg,ee}^{ij} - \Delta_{gg,eg}^{ij} - \Delta_{ee,eg}^{ij} \right)$$

$$i \left(\dot{\Delta}_{eg,gg}^{ij} \right)^0 = \Delta_{eg,gg}^{ij} (2E_{g,0} - E_{g,j} - E_{e,i}) + \quad (107f)$$

$$- \wp_{eg} \dot{y}_0 \left(2\Delta_{eg,eg}^{ij} - \Delta_{gg,gg}^{ij} - \Delta_{ee,gg}^{ij} \right)$$

$$i \left(\dot{\Delta}_{ee,ee}^{ij} \right)^0 = \Delta_{ee,ee}^{ij} (2E_{e,0} - E_{e,i} - E_{e,j}) + \quad (107g)$$

$$- \wp_{eg} \dot{y}_0 \left(2\Delta_{ee,eg}^{ij} - \Delta_{eg,ee}^{ij} - \Delta_{eg,ee}^{ji} \right)$$

$$i \left(\dot{\Delta}_{ee,eg}^{ij} \right)^0 = \Delta_{ee,eg}^{ij} (E_{g,0} + E_{e,0} - E_{e,i} - E_{e,j}) + \quad (107h)$$

$$- \wp_{eg} \dot{y}_0 \left(\Delta_{ee,gg}^{ij} + \Delta_{ee,ee}^{ij} - \Delta_{eg,eg}^{ij} - \Delta_{eg,eg}^{ji} \right)$$

$$i \left(\dot{\Delta}_{ee,gg}^{ij} \right)^0 = \Delta_{ee,gg}^{ij} (2E_{g,0} - E_{e,i} - E_{e,j}) + \quad (107i)$$

$$- \wp_{eg} \dot{y}_0 \left(2\Delta_{ee,eg}^{ij} - \Delta_{eg,gg}^{ij} - \Delta_{eg,gg}^{ji} \right).$$

A.2.2 Twin-atom beam generation

The equations of motion for the one-particle density matrices due to \hat{H}' , describing the emission process, are given by

$$i \left(\dot{\rho}_{gg}^{00} \right)' = \left\langle \left[\hat{a}_{g,0}^\dagger \hat{a}_{g,0}, \hat{H}' \right] \right\rangle = 0 \quad (108a)$$

$$i \left(\dot{\rho}_{ee}^{00} \right)' = -2i \sum_{ij} \kappa_{ij} \text{Im} \Delta_{gg,ee}^{ij} \quad (108b)$$

$$i \left(\dot{\rho}_{eg}^{00} \right)' = - \sum_{ij} \kappa_{ij} \Delta_{gg,eg}^{ij} \quad (108c)$$

$$i \left(\dot{\rho}_{gg}^{ij} \right)' = \sum_k \left(\kappa_{jk} \Delta_{gg,ee}^{ik} - \kappa_{ik} \left(\Delta_{gg,ee}^{jk} \right)^* \right) \quad (108d)$$

$$i \left(\dot{\rho}_{ee}^{ij} \right)' = 0 \quad (108e)$$

$$i \left(\dot{\rho}_{eg}^{ij} \right)' = \sum_k \kappa_{jk} \Delta_{eg,ee}^{ik} \quad (108f)$$

For the two-particle density matrices the equations of motion due to \hat{H}' are given by

$$\begin{aligned} i \left(\dot{\Delta}_{gg,ee}^{ij} \right)' &= \left\langle \left[\hat{a}_{g,i}^\dagger \hat{a}_{g,j}^\dagger \hat{a}_{e,0} \hat{a}_{e,0}, \hat{H}' \right] \right\rangle = \\ &\simeq \left(2\rho_{ee}^{00} + 1 \right) \sum_{kl} \kappa_{kl} \rho_{gg}^{ik} \rho_{gg}^{jl} - \kappa_{ij} \rho_{ee}^{00} \left(\rho_{ee}^{00} - 1 \right) + \\ &\quad - \rho_{ee}^{00} \left(\rho_{ee}^{00} - 1 \right) \sum_k \left(\kappa_{ik} \rho_{gg}^{jk} + \kappa_{jk} \rho_{gg}^{ik} \right) \end{aligned} \quad (109a)$$

$$\begin{aligned} i \left(\dot{\Delta}_{gg,eg}^{ij} \right)' &\simeq \rho_{eg}^{00} \sum_{kl} \kappa_{kl} \rho_{gg}^{ik} \rho_{gg}^{jl} - \kappa_{ij} \rho_{eg}^{00} \rho_{ee}^{00} + \\ &\quad - \rho_{eg}^{00} \rho_{ee}^{00} \sum_k \left(\kappa_{jk} \rho_{gg}^{ik} + \kappa_{ik} \rho_{gg}^{jk} \right) \end{aligned} \quad (109b)$$

$$i \left(\dot{\Delta}_{gg,gg}^{ij} \right)' \simeq - \left(\rho_{eg}^{00} \right)^2 \sum_k \left(\kappa_{jk} \rho_{gg}^{ik} + \kappa_{ik} \rho_{gg}^{jk} \right) - \kappa_{ij} \left(\rho_{eg}^{00} \right)^2 \quad (109c)$$

$$i \left(\dot{\Delta}_{eg,ee}^{ij} \right)' \simeq \left(2\rho_{ee}^{00} + 1 \right) \sum_{kl} \kappa_{kl} \rho_{eg}^{ik} \rho_{gg}^{jl} + \quad (109d)$$

$$- \rho_{ee}^{00} \left(\rho_{ee}^{00} - 1 \right) \sum_k \kappa_{jk} \rho_{eg}^{ik}$$

$$i \left(\dot{\Delta}_{eg,eg}^{ij} \right)' \simeq \rho_{eg}^{00} \sum_{kl} \kappa_{kl} \rho_{eg}^{ik} \rho_{gg}^{jl} - \rho_{ee}^{00} \rho_{eg}^{00} \sum_k \kappa_{jk} \rho_{eg}^{ik} \quad (109e)$$

$$i \left(\dot{\Delta}_{eg,gg}^{ij} \right)' \simeq - \left(\rho_{eg}^{00} \right)^2 \sum_k \kappa_{jk} \rho_{eg}^{ik} \quad (109f)$$

$$i \left(\dot{\Delta}_{ee,ee}^{ij} \right)' \simeq \left(2\rho_{ee}^{00} + 1 \right) \sum_{kl} \kappa_{kl} \rho_{eg}^{ik} \rho_{eg}^{jl} \quad (109g)$$

$$i \left(\dot{\Delta}_{ee,eg}^{ij} \right)' \simeq \rho_{eg}^{00} \sum_{kl} \kappa_{kl} \rho_{eg}^{ik} \rho_{eg}^{jl} \quad (109h)$$

$$i \left(\dot{\Delta}_{ee,gg}^{ij} \right)' = 0, \quad (109i)$$

where the factorization scheme $\langle ABC \rangle \simeq \langle A \rangle \langle B \rangle \langle C \rangle$ is used to approximate the three-particle density matrices.

B Coupled-cluster theory

B.1 Expectation values of excitation operators

The expectation values of the excitation operators, which appear in the cluster equations and are necessary to solve the system of coupled differential equations are

$$\langle \phi_0 | (\hat{S}^\dagger)^2 \hat{S}^2 | \phi_0 \rangle \simeq 2N(N-1) \quad (110a)$$

$$\langle \phi_0 | (\hat{S}^\dagger)^4 \hat{S}^4 | \phi_0 \rangle \simeq 4!N(N-1)(N-2)(N-3) \quad (110b)$$

$$\langle \phi_0 | (\hat{S}^\dagger)^2 \hat{S}^2 (\hat{S}^\dagger)^2 \hat{S}^2 | \phi_0 \rangle \simeq 4N^2(N-1)^2 \quad (110c)$$

$$\langle \phi_0 | (\hat{S}^\dagger)^6 \hat{S}^6 | \phi_0 \rangle \simeq 6!N(N-1)(N-2)(N-3)(N-4)(N-5) \quad (110d)$$

$$\langle \phi_0 | (\hat{S}^\dagger)^4 \hat{S}^2 (\hat{S}^\dagger)^2 \hat{S}^4 | \phi_0 \rangle \simeq 12 \cdot 4!N(N-1)(N-2)^2(N-3)^2 \quad (110e)$$

$$\langle \phi_0 | (\hat{S}^\dagger)^4 \hat{S}^4 (\hat{S}^\dagger)^2 \hat{S}^2 | \phi_0 \rangle \simeq 2 \cdot 4!N^2(N-1)^2(N-2)(N-3), \quad (110f)$$

where N is the total number of particles, $|\phi_0\rangle = |N, 0\rangle$ and $\hat{S} = \hat{a}_{e,0} \hat{a}_{g,p}^\dagger$.